Journal Of Marine Systems
July 2015, Volume 147 Pages 153-168
https://doi.org/10.1016/j.jmarsys.2014.10.003
https://archimer.ifremer.fr/doc/00351/46258/

Impact of increased grid resolution on global marine biogeochemistry

McKiver William J. [1,], Vichi Marcello [1, 3], Lovato Tomas [1], Storto Andrea [1], Masina Simona [1, 2]

[1] Ctr Euromediterraneo Cambiamenti Climat, Bologna, Italy.
[2] Ist Nazl Geofis & Vulcanol, Bologna, Italy.
[3] Univ Cape Town, Dept Oceanog, ZA-7700 Rondebosch, South Africa.

* Corresponding author : William J. McKiver, email address : william.mckiver@cmcc.it

Abstract :

Here we examine the impact of mesoscale processes on the global marine biogeochemical system by performing simulations at two different resolutions, 2 degrees (LO-res) and 1/4 degrees resolution (HI-res) using the PELAGOS model. Both the LO-res and HI-res simulations are set up with the same forcings and biogeochemical parameterizations, while the initial conditions are provided by a spinup of the LO-res simulation. This allows us to perform a direct inter-comparison of the two cases with a view to understanding how the introduction of mesoscale features affects the biogeochemical system, specifically how differences in the resolved horizontal and vertical motions are reflected in the plankton biomass and the nutrient availability. While the global large-scale oceanographic features (fronts, gyres, etc.) are captured in both the LO-res and HI-res simulations, differences in the mesoscale flow structures, and in particular the resolved vertical physics in the HI-res simulation generate very different behavior in the biogeochemical system. These differences in the physics drive what is a spun-up biogeochemical system in the LO-res simulation into a new regime in the HI-res simulation with significant reduction of typical low resolution biases. Coastal features are well reproduced due to stronger Ekman upwelling at the continental margins and increased eddy kinetic energy in the Southern Ocean significantly reduces the winter overestimation. These biases in the LO-res model are a result of inadequate vertical dynamics. The enhancement of surface chlorophyll can be attributed to improvements in the winter mixed layer in some regions such as the North Atlantic, while it is overall the difference in the Ekman vertical velocity which improves surface production allowing to simulate more realistic deep chlorophyll maxima as well. While the HI-res is better than the LO-res at capturing the timing of the spring bloom in the Southern Ocean, it still overestimates the peak of the bloom, hinting at the need to better understand the driving forces of the seasonal cycle of sub-Antarctic plankton dynamics.

Highlights

► Examine the impact of resolving mesoscale processes on global marine plankton ► Performed two simulations at 2° (LO-res) and 1/4° (HI-res) resolution ► Resolved vertical physics in the HI-res has a big impact on the plankton system. ► HI-res simulation significantly reduces typical low resolution biases. ► Coastal features are well reproduced due to stronger coastal Ekman upwelling.

Keywords : Marine plankton, Global ocean, Mesoscale processes, Chlorophyll, Nutricline

1. Introduction

The importance of marine plankton, both in terms of their role within the carbon cycle, as well as their position at the base of the marine food chain, has motivated great effort into understanding their evolution and distribution within the global ocean. Many observational studies have been conducted using in-situ measurements from ship cruises (*Srokosz* [1997], *Kang et al*. [2004], *Gist et al*. [2009]), as well as satellite observations (*McClain et al*. [1998], *Gregg et al*. [2003], *McClain* [2009]) to understand the large scale distribution of plankton. While there has been a marked increase in these observational studies in recent years, limitations in obtaining measurements in the global ocean have naturally led to a greater dependence on computation models, and with increasing computational power more complex models at ever greater resolution have been employed.

Many global biogeochemical models can now resolve the large scale dynamics, incorporating the effects of the Earth's rotation, solar heating and wind forcing (*Moore et al*. [2002], *Griffies et al*. [2005], *Oke et al*. [2013]). These models, while being able to capture the basic largescale distribution of plankton when compared with satellite observations, still contain many biases at the regional scales, with each model having weaknesses in one region or another

(*Vichi & Masina* [2009]; *Friedrichs et al*. [2009]; *Doney et al*. [2009]). These biases may be due to an inadequete representation of the biogeochemical system, either through the use of an over-simplified plankton model or inaccurate parameterizations. However another important factor in these observed biases may be under-resolved physical scales. Recent regional studies have pointed to the importance of mesoscale ($\sim O(10-100km)$) and submesoscale ($\sim O(1-10km)$) features in shaping the distribution of marine plankton (*Lévy et al*. [2012], *Lévy & Martin* [2013]). Therefore while increasing the complexity of the biogeochemical model may be one way to correct biases, it is also important to understand what effect resolving more of the physical scales have on the biogeochemical system. Here we apply the latter approach, by comparing the same biogeochemical model applied at two different resolutions.

It has been shown that as models resolve the mesoscale and submesoscale one sees stronger vertical motions (*Mahadevan & Tandon* [2006], *Lévy* [2008]). Despite the fact that at the mesoscale the vertical motions are still very weak compared to the horizontal components ($\sim 1/1000th$) the biogeochemical system is extremely sensitive to even small changes in this crucial field. However what is still not clear is how this resolved physics impacts the biogeochemical system on the large scale. In particular, do these resolved scales with greater vertical transport strength and variability have a positive or negative impact on the overall productivity of the phytoplankton community. Many different studies have found conflicting answers to this question. *Oschlies* [2002] found a strong negative eddy-driven vertical advection in the flank of the North Atlantic subtropical gyre that resulted in decreased production, while *McGillicuddy et al*. [2003] did not confirm this but found a large downward nutrient flux in the sub-polar region with a substantial impact on growth. The reduction of primary production appears to be a more robust response when mesoscale to sub-mesoscale processes are included. *Lévy et al*. [2012]b considered a regional model applied to the North Atlantic and North Pacific subtropical gyre where they found that going from mesoscale-resolving ($1/9°$) to sub-mesoscale ($1/54°$) scales led to an overall decrease in phytoplankton abundance. However, *Karleskind et al*. [2011] found little changes in primary production in a North Atlantic 4.5 km resolution simulation when compared with a version of the model with the same resolution but stronger eddy diffusivity.

Most models employed to study the ocean biogeochemical system have had to compromise, either in the resolved physical scales used or the biogeochemical complexity of the model, and often when more of the physical scales are resolved the model is only applied at regional scales (*Gruber et al*. [2011], *Lévy et al*. [2012], *Mahadevan et al*. [2012]). Here we try to make as realistic an implementation of the global ocean biogeochemical system as possible, by employing a sophisticated biogeochemical model, the Biogeochemical Flux Model (BFM, *Vichi et al*. [2007a], b), coupled to the NEMO ocean model (*Madec et al*. [1999]) at $1/4°$ resolution. We perform simulations at two different resolutions: (1) $2°$ (LO-res) and (2) $1/4°$ (HI-res). The $2°$ is capable of resolving scales greater than 60 km, whereas the $1/4°$ resolves scales of greater than 10 km. These resolutions were chosen because they represent the transition between the current resolutions of the Earth System Models (ESM) used for climate change impacts and future projections in the Climate Model Intercomparison Project phase 5 (CMIP5, with ocean models between 1 and 2 degrees) and the kind of planned resolutions for the next generation of ESMs. The proposed HI-res model is not yet eddy-resolving although it allows to directly compare the impact of including the mesoscale with respect to a model that only resolves the largescale (LO-res). However while the LO-res case is spun-up, only the physics of the HI-res is spun-up, with the biology initialized from the LO-res. Thus we can examine directly how this spun-up biology, produced within the LO-res, reacts to the resolved dynamics in the HI-res.

In the following section we describe the model and simulations setup used, as well as providing a list of observation data used for comparison with the model. In section 3 we present the results, first considering the differences in the physics at the two resolutions in Section 3.1, then presenting an overview of the differences in the seasonal chlorophyll production in Section 3.2, followed by closer analysis of the impact of resolved scales on the biogeochemical system in different regions. Finally we discuss the consequences and draw our conclusions in Section 4.

2. Methods

2.1. Model and simulation setup

Here we use the PELAGOS (PELAgic biogeochemistry for Global Ocean Simulations, (*Vichi et al*. [2007a], b), which is a coupling between the NEMO general circulation model (version 3.4, www.nemo-ocean.eu, *Madec et al*. [1999]) and the Biogeochemical Flux Model (BFM, version 5, http://bfm-community.eu). The BFM model is based on a biomass continuum description of the lower trophic levels of the marine system. The model implements a set

of biomass-based differential equations that solves the fluxes of nutrients (carbon, nitrogen, phosphorus, silicate and iron) among selected biological functional groups (phytoplankton, zooplankton and bacteria) representing the major components of the lower trophic levels. The functional groups are further subdivided in implicitly size-based groups, namely diatoms, nanoflagellates and picophytoplankton for primary producers, heterotrophic nanoflagellates, microzooplankton and mesozooplankton for the predators. Another peculiarity of the model is that the nutrient stoichiometry is not fixed and therefore the ratios of carbon to N, P and Si can vary within the living functional groups as well as the chlorophyll to carbon ratio in phytoplankton (see *Vichi et al*. [2007a] and *Vichi et al*. [2014] for a full description of the equations). In all we have 52 pelagic state variables with diagnostics.

The PELAGOS model is applied at global scale with two different resolutions, 2° ($n_x \times n_y = 182 \times 149$, LO-res) and 1/4° ($n_x \times n_y = 1442 \times 1021$, HI-res) on an ORCA grid (*Madec & Imbard* [1996]). The 2° grid has a nominal resolution of 2° with a refinement of the latitudinal grid size towards the equator down to 0.5°, whereas the 1/4° grid gets finer with increasing latitude, going from an effective resolution of 28 km at the Equator to 10 km at the Poles (*Barnier et al*. [2006]). The LO-res has 31 vertical levels, while the HI-res has 50 vertical levels, each having 10 and 22 levels spanning the upper 100 m respectively. A timestep of 96 minutes and 18 minutes are used for the LO-res and HI-res respectively. Both implementations use the same biogeochemical parameterizations and both are coupled to the LIM2 sea-ice model (*Fichefet & Morales Maqueda* [1997], *Bouillon et al*. [2009]). The physical parameterizations for the LO-res are as in *Vichi et al*. [2007b] and *Vichi & Masina* [2009], whereas for the HI-res they follow closely the DRAKKAR ORCA025 configuration (*Barnier et al*. [2006]). In the LO-res model lateral momentum is diffused with a Laplacian operator whereas a bilaplacian is applied in the HI-res model, each of them using a viscosity coefficient of 40000 m^2s^{-1} and -1.5×10^{11} m^2s^{-1} respectively. However for the LO-res also an eddy-induced velocity scheme is used to parameterize subgrid processes (*Gent & McWilliams* [1990]). For both the LO-res and HI-res cases a Laplacian operator is used to diffuse tracers (temperature, salinity and biogeochemical tracers) with a diffusivity coefficient of 2000 m^2s^{-1} and 300 m^2s^{-1} respectively. Vertical eddy diffusion of momentum and tracers is parameterized with a Turbulent Kinetic Energy (TKE) closure scheme (*Blanke & Delecluse* [2009]) with eddy viscosity and diffusivity coefficients of 1.2e-4 m^2s^{-1} and 1.2e-5 m^2s^{-1} respectively. The surface of the ocean is forced using ERA-INTERIM reanalysis data (*Dee et al*. [2011]), which is the latest global atmospheric reanalysis produced by the European Centre for Medium-Range Weather Forecasts (ECMWF), and provides daily forcing values for snowfall, precipitation, surface solar and thermal radiation, and 3-hourly forcing for 10 m wind velocity components, 2 m temperature and the specific humidity. The temperature and salinity are initialized using the World Ocean Atlas data interpolated on the model grid (*Levitus* [1982]), with both being relaxed to climatological values. The model includes nutrient river inputs (from *Cotrim da Cunha et al*. [2007]) but no benthic remineralization.

In the case of the LO-res the fully coupled system (BFM plus NEMO) was spun-up for over 15 years, starting in the year 1982, with the biological variables being initialized with uniform values. For the HI-res case only the physical model was spun-up for 10 years beginning in the year 1989. It was then coupled to the biogeochemical model using the biogeochemical variables interpolated from the LO-res experiment to initialize. Then both the LO-res and HI-res cases were run for 2 years (1999, 2000). This allows us to not only compare the seasonal cycles in the two cases but also assess how well the biological conditions have adjusted in the HI-res case.

2.2. Observational data

We used a number of publicly available observational datasets to compare with the model results. Where data has not been available during the period of the simulation run we have opted to use climatological data (as in the case of the mixed layer depth).

(i) Mixed layer depth (MLD) climatologies have been obtained from data based on Argo profiling floats and using a 0.2°C temperature criterion (*Hosoda et al*. [2010]). This data uses 10 day profiles collected between 2001 and 2009 to construct MLD data on a $1^\circ \times 1^\circ$ regular grid.
http://www.jamstec.go.jp/ARGO/argo_web/MILAGPV/index_e.html

(ii) Chlorophyll data is obtained from NASA satellite derived monthly composites from the Sea-viewing Wide Field-of-view Sensor (SeaWiFS) data (level 3 products) at 9km resolution and for the period of the model simulation, beginning 1999 till the end of 2000.
http://oceandata.sci.gsfc.nasa.gov/SeaWiFS/

(iii) In situ chlorophyll and phosphate data have been obtained from the World Ocean Database and phosphate climatological data from the World Ocean Atlas set of objectively analyzed 1° gridded climatological fields (*Garcia et al*. [2010])

(iv) Measurements of temperature, salinity, phosphate and chlorophyll in the Southern Ocean from the MD166 BONUS-GoodHope cruise in February-March 2008 (*Arhan et al*. [2011]; *Le Moigne et al*. [2013]).

3. Results

3.1. Physical drivers

Before examining the impact of resolution on the biogeochemistry, we first compare and contrast the physics in the two experiments. Beginning in Figure 1 we plot the mean sea surface temperature and sea surface salinity values averaged over the entire 10 year spin-up for the LO-res and HI-res. The ORCA2 grid is largely used in global ocean simulations and coupled climate models because of its ability to resolve the large scale features and equatorial processes particularly in the Pacific Ocean. Indeed, there is very little difference in the surface ocean features of the two model resolutions, with the location of most large scale fronts being the same. A more quantitative comparison of the two model cases with observed data on a Taylor diagram (not shown) reveal that both cases have a high correlation with the observations and are virtually indistinguishable one from the other. However, there are some regional differences in the sea-surface salinity, namely, in the Indian Ocean where lower salinity tongue extends further westward in the HI-res case and in parts of the Southern Ocean, where salinity is higher in the HI-res.

In Figure 2 we compare climatologies of the mixed layer depth (MLD) in the two simulations based on $0.2°C$ temperature criterion spatially averaged in four regions: (a) the North Atlantic, (b) the Tropical Atlantic, (c) the Southern Ocean and (d) the South Pacific. Also we plot observed climatologies based on the data set from Argo profiling floats (*Hosoda et al*. [2010], Sec. 2.2). In all cases the HI-res better represents the observed MLD having overall a deeper MLD than the LO-res. However, both of them tend to under-estimate the observed MLD, particularly during the summer periods when strong stratification occurs in the model. In the Southern Ocean the HI-res over-estimates the winter MLD, but is still much closer to the observations than the LO-res. In a work using a previous version of the PELAGOS model at 2° resolution (*Vichi & Masina* [2009]) they have shown the importance of deep mixing for regulating the Southern Ocean bloom and identified the early stratification as being responsible for the high chlorophyll bias they found in the model. The HI-res model is however still deficient in the simulation of the onset of the seasonal stratification, as while the maximum winter mixing is much better reproduced, the slope is steeper than observed and leads to the same MLD values of the LO-res in the period from September to December.

The aim of this work is to assess the importance of resolved scales when using the same external forcing functions. It is then important to consider how the energy varies in the two cases. Momentum is put into the system through the scalar wind stress which is identical in both cases and simply interpolated to different grids. Both the LO-res and HI-res cases converts a certain amount of this into kinetic energy at their own resolved scales. In Figure 3a we show the ratio of the total average kinetic energy (KE) computed over the entire model domains and the wind stress for both the LO-res and HI-res during the spin-up phase. In both cases the energy quickly equilibrates, with the HI-res having over twice the KE relative to the wind stress, and thus is a much more energetic system than the LO-res, with much more of the wind stress converted into kinetic energy. Also as an indicator of the relative importance of the vertical motions in the two simulations in Figure 3b we show the global spatial average of the ratio of the magnitude of the vertical-to-horizontal motions. As is the case for the kinetic energy, the vertical velocity is much stronger in the HI-res simulation, indicating that despite the large similarity in the temperature and salinity surface fields shown in Fig. 1, there is a substantial increase in vertical motion that is going to affect the biological variables in the upper ocean (Sec. 3.2).

Wind stress is not affected by resolution, however wind curl is and vertical transport in the upper layer is affected by curl as theoretically derived by *Ekman* [1905]. In Figure 4 we show the mean Ekman vertical velocity (upwelling and downwelling) computed from the wind-stress for both the LO-res and HI-res. As it occurs for the other surface mean properties at the larger scales, overall the wind driven vertical transport is similar in both magnitude and spatial variability to the LO-res. There are however more fine scale features in the HI-res that become particularly intensified at coastal regions where the LO-res model is necessarily unable to resolve the spatial features as it will be further analyzed in Sec. 3.2.2. In summary, the use of an eddy-permitting model in contrast to a coarse resolution model

leads to expected differences in the physics, which can be quantified in higher kinetic energy and vertical motions, stronger Ekman transport in coastal regions and an overall deeper mixed layer depth during the winter periods.

3.2. Biological response

3.2.1. Surface chlorophyll

Now we examine how resolution impacts the simulated biological system. In Figure 5 we show colourmaps of the monthly mean surface chlorophyll concentration in March, June, September and December of the second year, 2000, for the LO-res and HI-res simulations, with colourmaps of the monthly mean SeaWiFS satellite data in the same year. Here we use chlorophyll as an indicator of surface biomass allowing comparison with satellite estimates. We chose surface chlorophyll to fix the reference depth, in contrast to *Vichi et al*. [2007a] where they used vertically integrated chlorophyll (note that the LO-res chlorophyll comparison with observations improves when the vertically integrated value is used accordingly to *Vichi et al*. [2007a]). Substantial differences in the LO-res and HI-res experiments are visible even at the beginning of the first year 1999 (not shown) and they persist throughout the second year with higher biomass in the equatorial and coastal regions in the HI-res, while the Southern Ocean biomass is reduced compared to the LO-res. In the austral winter the high biomass bias that occurs in the LO-res in the southern subtropical gyres is strongly suppressed in the HI-res. Biomass in the Southern Ocean increases again in September, with the chlorophyll concentration in the HI-res being comparable to the LO-res in December.

In order to have an objective measure of the comparison between the model and observation surface chlorophyll we compute the Nash-Sutcliff Model Efficiency index (*Nash & Sutcliffe* [1970]), which is a measure of the ratio of model error to the variability of the observations:

$$MEF = 1 - \frac{\sum_{n=1}^{N}(O_n - P_n)^2}{\sum_{n=1}^{N}(O_n - \overline{O})^2}. \tag{1}$$

where O_n and P_n are the N pairs of observational data and predictions, respectively. Performance levels are usually categorised as follows: > 0.65 excellent, $0.65 - 0.5$ very good, $0.5 - 0.2$ good,< 0.2 poor. If the index is lower than 0, it means that the model is a worse predictor than the mean of the observations. Values around 0 indicate that the model captures the spatial mean but has a poor to good representation of the variability. In Figure 6 we show the MEF index computed for both the Northern and Southern Hemisphere so that we can see the seasonal dependence. For both the LO-res and HI-res the model skill is much higher in the Northern Hemisphere, with the LO-res having a slightly higher skill level during the summer, but sharply dropping during the winter period. In the Southern Hemisphere the HI-res is much better, again particularly during the winter period. However towards the end of the simulation the skill level of the HI-res is dropping, probably as a result of the return of the high chlorophyll bias in the Southern Ocean as was seen in December in Figure 5. Despite this drop it still has a higher skill level than the LO-res.

The skill improvement in the Northern Hemisphere winter of the HI-res hints at a better representation of the winter-spring bloom. Indeed, the MLD in the whole North Atlantic is much more in accord with the observations (Fig. 2) and this has an impact on surface chlorophyll. In Figure 7 we computed the mean surface chl concentration over in the North Atlantic for both simulations and compared it with the satellite data. The enhanced mixed layer does increase the spring bloom in the HI-res and improves the timing with a better representation of the summer decay, though the main peak is now overestimated. The use of an eddy-permitting resolution generally enhances the production in the North Atlantic with respect to a simulation that only resolves the large scale circulation.

In the following sections we take a closer look at the differences in the two resolutions, focussing on four specific regions: coastal, equatorial, subtropical gyres and the Southern Ocean. Within each region we examine timeseries in the sample boxes indicated in Figure 5.

3.2.2. Coastal

One of the main differences that resolved scales produces is a strong enhancement in the coastal chlorophyll that is an evident feature in satellite images. The mechanism at the base of this enhancement is clearly seen in Figure 8 where we show the Ekman vertical velocity and chlorophyll concentration for three coastal regions in the Northern Hemisphere: (a) the Eastern North Pacific, (b) the Western North Atlantic and (c) the Eastern North Atlantic. The coastal biomass in the HI-res is boosted by the presence of a strong Ekman driven coastal upwelling which is not resolved in the LO-res case. In Figure 8(a) we can see this enhancement in the Californian Coastal Current. There

is however a reduction in the offshore chlorophyll driven by eddy transport of nutrients into the open ocean as was seen in *Gruber et al*. [2011]. The Gulf Stream region in Figure 8(b) is characterized by the transport of upwelled nutrients from the coastal region into the North Atlantic drift. Upwelling is much enhanced in the HI-res which brings up more nutrients from the southern subtropical sources (*Palter & Lozier* [2008]). However, in the annual average the offshore chlorophyll does not seem to be increased much by this transport (through nutrient advection as has been seen in *Pelegrí & Csanady* [1991] and *Pelegrí et al*. [2006]), but only closer to the coast. In Figure 8(c) showing the eastern part of the North Atlantic we see stronger upwelling in the HI-res. The wind forcing causes a near shore Ekman transport which induces upward vertical motions that bring nutrients from deep into the euphotic zone where they can sustain high chlorophyll concentrations (*Pelegrí et al*. [2005], *Pelegrí et al*. [2006]). In this coastal region the Ekman upwelling plays a much stronger role than the MLD in providing nutrients to the surface as was shown in *Pastor et al*. [2013].

To further understand the effect this enhancement in coastal upwelling has on the biological system we focus on one example in the Eastern North Atlantic, at the Senegal coastline. In Figure 9 we plot a cross section at 13°N and compare the LO-res, HI-res annual means to phosphate and chlorophyll concentrations from the World Ocean Database (Sec. 2.2). The paucity of data does not allow to compute an annual mean of the observations and they have been plotted independently of the season. The observed phosphate concentration is much higher than seen in both the simulations, which are rather similar, indicating how the LO-res spin up sets the initial state of pre-formed nutrients. There is a much diffused nutricline in both the simulations that is not found in the observations, though the HI-res is shallower than the LO-res case (see also Fig. 10). Despite the rather similar vertical structure of the macro-nutrients, the response of the simulated phytoplankton is different. The composed chlorophyll data shows a strong subsurface signal at 50 m with a surface maximum on the coastal shelf. The LO-res bloom is much deeper and completely lacks the surface bloom along the coast as the shelf is not resolved. The deep chlorophyll maximum (DCM) is flat at around 100 m with only a slight surface increase towards the coast. This is instead better captured in the HI-res, though the intensity of the coastal bloom is much weaker than observed. One distinctive feature in the HI-res case, is the appearance of a double maximum in the chlorophyll, one just under 50 m and the second centered below 100 m. The split in the chlorophyll maximum is due to different responses by the two main phytoplankton groups, diatoms and flagellates, to the increased nutrient supply. While diatoms are able to take advantage of the available nutrients, blooming at shallower depths in the HI-res and escaping the predation pressure, the bloom in flagellates remains confined to deeper waters where nutrients are steadily more abundant. This is more similar to the LO-res case where both flagellates and diatoms have deep maxima. There is no evidence of a double maximum in the data, therefore this response is to be seen as a partial adjustment of the HI-res biology to enhanced nutrient supply. Notwithstanding the partial increase of vertical upwelling due to the improved resolution, it is clear that the HI-res is not capable to change substantially the vertical structure of nutrients determined by the spin up done with the LO-res.

We also analysed time series of selected variables within a 6×6 degree grid box, centered at 18°W, 13°N (Fig. 10, see the box location in Fig. 5). This allows us to study the surface seasonal cycle using satellite chlorophyll data as well as further investigate the adjustment time scales for the HI-res case when initializing from the spun-up initial conditions from the LO-res. Both the LO-res and the HI-res start from the same values but in 5 days are rapidly changed. The nutricline in the HI-res slowly stabilises around 50 metres, much shallower than the LO-res depth at 90 m and much closer to the observed value of 30 m. This value is not yet adjusted after the 2 years of HI-res simulation and it is slowly moving upward. This is an indication of the more active vertical dynamics of the HI-res, which are however insufficient to recover the deep nutricline initially set by the LO-res. As seen in Fig. 9, the DCM in the HI-res adjusts to a much shallower level, going from about 90 m to 40-50 m which is in accord with the available data. Comparing the MLD, we see a slightly deeper MLD in the HI-res with respect to the LO-res, being closer to the observed climatology. Though the phosphate at the surface in both cases are similar, the shallower nutricline in the HI-res case indicates that there are more nutrients available closer to the surface. This is driven by a stronger Ekman vertical velocity, where the large peaks in the Ekman upwelling correspond with shallowing of the nutricline and the DCM. Observed phosphate concentrations at the surface are much higher throughout the seasonal cycle giving rise to high peaks in the chlorophyll concentration during the spring bloom period. These peaks are still absent in the HI-res case despite the relevant shallowing of the DCM shown in Fig. 9 and 10. The HI-res case is relatively better having higher concentrations of chlorophyll through the increased nutrient availability, but the high surface levels are not that evident at this coastal longitude as seen in the observations.

Similarly the DCM in the HI-res also adjusts to a much shallower level, going from about 90 m to 40 m. Comparing

the MLD, we see a slightly deeper MLD in the HI-res with respect to the LO-res, being closer to the observed climatology. Though the phosphate at the surface in both cases are similar the much shallower nutricline in the HI-res case, indicate that there are more nutrients available closer to the surface. This is driven by a stronger Ekman vertical velocity, where the large peaks in the Ekman upwelling correspond with shallowing of the nutricline and the DCM. Observed phosphate concentrations at the surface are much higher throughout the seasonal cycle giving rise to much higher peaks in the chlorophyll concentration during the spring bloom period. Though surface chlorophyll in both cases under-estimate the observations, the HI-res case is much better having higher concentrations of chlorophyll through the increased nutrient availability.

3.2.3. Equator

We now turn our attention to the Equator, another region where surface biomass improves in the HI-res case as can be seen in Figure 5 where the HI-res substantially enhances the Equatorial upwelling blooms. In particular the Equatorial Pacific is well captured in the HI-res, though the underestimation in the eastern part is still present. In Figure 11 we plot cross sections of the annual mean phosphate as an example of macronutrients and chlorophyll for the equatorial Pacific from the two simulations as well as observations from the World Ocean Database (Sec. 2.2). The mean annual shape of phosphate is characterized by a surface minimum close to the Ecuadorian coast and a marked eastern upwelling that follows the thermocline with a progressive deepening of the 1 μmol m^{-3} isoline from 50 to about 150 m in the western part. Chlorophyll distribution however does not follow this feature with a maximum that is located at 50 m depth at all longitudes (*Pennington et al*. [2006]). The degree of patchiness in chlorophyll is connected to the data sparsity and it may be smoothed by the choice of the correlation radii in the objective analysis tool (DIVA, *Troupin et al*. [2012]). The HI-res simulation improves the distribution of phosphate both in terms of shape and concentration, although the underestimation is still evident. The higher resolution allows to resolve the Galapagos Islands and the discontinuity with the minimum on the eastern part. Similarly the sub-surface chlorophyll maximum is more similar to observations in the HI-res, with biomass even reaching the surface in the western half of the cross section. This is more like the observations which has more chlorophyll closer to the surface, and extending down only to depths of 100 m. The eastern part closer to the Galapagos is however still underestimated as the coastal upwelling of nutrients is not correctly reproduced also at the higher resolution.

In Figure 12 we plot timeseries of surface chlorophyll and phosphate, as well as the sub-surface chlorophyll maximum, nutricline, MLD and depth averaged vertical velocity, all spatially averaged within a 6 by 6 degree in the Equatorial Pacific centered at $100°W, 0°N$ (see Fig. 5) to study the adjustment of the HI-res simulation starting from the LO-res initial conditions. There is very little difference between the MLD in the two cases, both being much shallower than the observed values, although the HI-res is marginally deeper during the deepest mixing period. Chlorophyll however is much higher in the HI-res, being much closer to the observations. This is due to an upsurge in nutrient supply as indicated by the shallowing of the nutricline as was shown in the section in Fig. 11. These nutrients are quickly taken up with phosphate concentrations remaining similar in both cases at the surface. Apart from an initial adjustment the nutricline in the HI-res remains relatively stable at 40 m in good agreement with the observations, unlike the LO-res case where the nutricline is much deeper and has very strong seasonal dependence, getting as deep as 100 m during the deep mixing period. Also the DCM is much shallower in the HI-res case. After an initial adjustment in the first 2 months the chlorophyll maximum in the HI-res stabilises at a depth of 45 m, as seen in the observations, whereas the LO-res oscillates about 80 m. Though the Ekman vertical velocity cannot be computed at the equator, a stronger wind driven meridional component in the HI-res (not shown) lead to an overall stronger vertical upwelling and downwelling as can be seen in the timeseries of the depth-averaged vertical velocity. This stronger wind-driven velocity in the HI-res case supplies more nutrient which maintain the higher surface phytoplankton.

3.2.4. Subtropical gyres

Next we turn to places where the HI-res has much lower chlorophyll concentration with respect to the LO-res, beginning with the subtropical gyres. The subtropical gyres are the oceanic regions with the lowest chlorophyll concentration (Fig. 5). The LO-res and generally most of the biogeochemical models tend to overestimate production in these regions (e.g. *Vichi & Masina* [2009]; *Doney et al*. [2009]; *Saba et al*. [2010]). Our results show that, despite the conventional knowledge of these regions being dominated by large-scale, low-frequency processes, the increased resolution reduces phytoplankton biomass respect to the LO-res. In Figure 13 we plot timeseries averaged in a 6 by 6 degree box located in the Southern Pacific subtropical gyre, centered at 123°W and 27°S. In this region observations

indicate a low chlorophyll concentration with little seasonality as a result of the permanently deep nutricline but also the presence of deeper winter mixing that contribute to maintain a relatively high mean value of phosphate concentration around 0.13 μmol m^3. The HI-res simulation produces deeper mixed layer depth during the winter periods, following much more closely the observed values. It is particularly the vertical motion that is enhanced, by means of high-frequency variability with intense upwelling events during the winter period which leads to much higher nutrient levels with respect to the LO-res. After an initial adjustment of about 7 month the nutricline stabilises at just above 300 m, much deeper than the LO-res, but still without the ability to simulate the climatological deepening at the height of the deep winter mixing periods. Surface chlorophyll in the HI-res is much lower being much closer to the observations and with a substantial reduction in seasonal variability. Here the contrast in the two simulations is even more stark, as the blooms in diatoms are significantly reduced and completely out of sync, peaking in August in the LO-res, while shifting to March-April in the HI-res. However while the chlorophyll concentrations in the HI-res are much more similar to the very observed low concentrations, the seasonal cycle seems to be more out of phase. This may be a problem of having to adjust from the initial high concentrationns developed in the LO-res spinup.

3.2.5. Southern Ocean

Finally we consider the Southern Ocean where again the bloom seen in the LO-RES is now suppressed in the HI-res case (see Figure 5). Observations in the Southern Ocean are less abundant than in other regions and characterized by gaps in the coverage of the seasonal cycle due to the difficulties of sampling during the Austral winter. We have preferred to focus the simulation assessment on the comparison with one single cruise data to preserve the frontal features instead of building a climatology from a series of sparse observations over a large time span that would have smeared out the spatial distribution. As introduced in Sec. 2.2, we used the high-resolution sampling data from the BONUS-GoodHope cruise in summer 2008 as a typical example of well-developed bloom conditions to check the role of resolved scales in shaping the nutrient and phytoplankton distribution across the polar front. These data are similar to the features found in other cruises on the GoodHope line over the same sampling period (*Swart et al.* [2012]). In Figure 14 we show the comparison of the depth profiles of temperature and salinity from these data with the LO-res and HI-res results over the same period in order to see how well the models resolve the front. The front is marked by a sharp decrease in temperature and salinity going from the subtropical gyre southwards towards the Antarctic Circumpolar Current and is usually identified by means of subsurface properties (*Orsi et al.* [1995]). In the observations this front occurs at about 44S, while there is stark differences in the two model cases, with the HI-res being a much more sharp transition, though occuring slightly north of the observed front, while the LO-res front is much more diffuse. Also the HI-res has stronger variability in the MLD relative to the LO-res, more characteristic of the observed MLD, reflecting the greater variability in the deep mixing of both the temperature and the salinity. In Figure 15 we show the comparison for phosphate and chlorophyll. Here we see the front marking a sharp transition in the nutrient availability, with very low phosphate within the subtropical gyre, but a sharp increase as you cross the front moving South. As was the case with the physical variables this transition is much better captured in the HI-res case, with much higher phosphate concentration beyond the front. The near surface chlorophyll is also better captured in the HI-res, with the maximum value occuring north of the front as in the observations, and a steep decline in chlorophyll beyond the front, whereas the LO-res shows a high bias beyond the front. However at depth the HI-res over-estimates the observed chlorophyll, indicating that the high chlorophyll at the surface in the LO-res is now being mixed deeper in the water column.

As before in Figure 16 we look at the timeseries within a box region centered at 0°W, 47°S (Fig. 5) to see the seasonal cycle of selected variables. Overall the chlorophyll concentration is much lower in the HI-res case, with diatoms being surpressed during the winter period. This is driven by a much deeper MLD in the HI-res during this period, while providing more nutrients to the surface, limits the light available to the phytoplankton inhibiting growth. However during the summer months when the ocean restratifies a much stronger bloom occurs in the HI-res with the growth in diatoms being much higher. This is due to the greater availability of nutrients that have been built up at the surface during the winter period. Also the timing of the bloom period is different in the two cases with the peak of the bloom shifting from August in the LO-res to October in the HI-res, yet not reaching the December bloom of the satellite. Again this follows the MLD which takes longer to restratify in the HI-res, occurring approximately one month after the LO-res. Surface phosphates are much higher in the HI-res closer to the observations. The nutricline in the HI-res is completely correlated with the evolution of the MLD. Overall we see a situation which is in stark contrast to the coastal regions, where Ekman transport has a strong impact. Instead here it is the very deep mixed layer depth,

driven by strong vertical motions in the HI-res that give rise to much deeper mixing. While this provides the large concentration of nutrients at the surface, the biomass and chlorophyll concentration is significantly reduced as a result of downwelling to depths where light is limited.

4. Discussion and conclusions

In this work we examined marine plankton in the global ocean using a model of the lower trophic marine system fully coupled to an ocean model implemented at two different resolutions, 2° (LO-res) and 1/4° (HI-res). We performed two simulations, the first at 2° resolution using the fully coupled model for 18 years. The second simulation was at 1/4° degree resolution where due to the computational limitations we only spun up the physics for 10 years, and then using the biological variables interpolated from the LO-res case we ran this coupled model for two more years. Analysis of the physics of both simulations revealed, while the sea-surface temperature and salinity are comparable, there are huge differences in the kinetic energy and the mixed layer depth in the two models. Since the HI-res is much more energetic and has much stronger vertical physics than the LO-res this leads to much deeper mixed layer depths, and with much more rapid re-stratification that leads to the improvement in the timing of the bloom (for example in North Atlanctic, see Fig. 7). However it is likely that with the tested resolutions we only see an enhancement of the mean flow and turbulent mixing without the effective dynamics of the mesoscale and sub-mesoscale processes that are needed to better capture the re-stratification (*Mahadevan et al*. [2010]). Also Ekman wind driven velocities are overall similar except at coastal regions where they are stronger in the HI-res. These differences in the physics give rise to strong differences in the biogeochemical variables, which drive what is a spun-up biogeochemical system in the LO-res into a new regime in the HI-res simulation where there is overall greater nutrient availability, much higher primary production along coastlines and at the equator, while growth is suppressed in the Southern Ocean and within the subtropical gyres. An objective comparison of the simulated surface chlorophyll with satellite using the Model Efficiency index (*Nash & Sutcliffe* [1970]) revealed that the HI-res is a much better representation of the observed chlorophyll concentration in the Southern Hemisphere, while in the Northern Hemisphere the HI-res is only superior during the winter period. Focusing on a few different regions we were able to uncover the different mechanisms at work in creating the differences between the two simulations. Overall as we move to the higher resolution we begin to see mesoscale processes with stronger vertical dynamics, as well as better resolved topographic features, and stronger Ekman velocities. It has been shown that these mechanisms have a stronger or weaker impact on the biogeochemical system depending on the region of the ocean. However the complete attribution of these mechanisms to specific processes is not straightforward and determining the specific impact of each one has been left to future work.

In coastal regions we found that stronger Ekman suction in the HI-res with respect to the LO-res can maintain growth as more nutrients are present within the shallow water. Though we also see some off-shore reduction in chlorophyll in the HI-res case off the California Current. Here we may have a mixture of Ekman driven upwelling and mesoscale dispersion of nutrients, with enhancement of coastal upwelling because of the scale resolution but depression of biomass because of eddy dissipation of nutrients in the off-shore region. The same mechanism was shown in *Gruber et al*. [2011] where they found that eddies produce an overall decrease in chlorophyll in this region. *Lathuilière et al*. [2011] also found that mesoscale processes can decrease chlorophyll, not only because of the dissipation of nutrient supply, but also because of the subduction of chlorophyll by downward vertical velocities, the mechanism for which was further illicited in *Lathuilière et al*. [2011]. However in these studies they compared the effect of eddies where there is already coastal upwelling, in the case of *Gruber et al*. [2011] by removing the non-linear advective term in the momentum equations and finding that the presence of eddies acts to reduce overall the primary production. In our case it is the very strong enhancement of Ekman driven upwelling going from the LO-res to the HI-res that is the dominant mechanism in giving an overall increase in chlorophyll. All coastal maxima are better reproduced in the HI-res than in the LO-res without the need to include any additional local parameterization such as nutrient bottom fluxes or restoration to nutrient climatological values. Since overall the evolution of the MLD is very similar in the two cases, it is clear that here it is the difference in the Ekman vertical velocity which is the main driver in generating more biomass at the surface in the HI-res case. Even so the HI-res still very much under-estimates the observed chlorophyll values (see for instance Figure 10). The vertical enhancement is not sufficient to overcome the shortage of surface nutrients imposed by the initial state of the nutricline from the LO-res. There may be a problem of an initial condition adjusted to low availability of surface nutrients, implying the need to have a spin up with the HI-res, though

the computational cost for such a spin up is very high and more efficient methods other than just interpolation from a coarse grid should be sought for.

In the Equatorial regions again wind driven motions generate stronger vertical upwelling in the HI-res with respect to the LO-res, producing a shallower nutricline and boosting chlorophyll production at the surface. Comparison with observations show that the HI-res performs better than the LO-res, with the nutricline depth very similar to the observed climatology, while surface chlorophyll is slightly over-estimated. This over-estimation by the HI-res seems to be a persistent feature throughout the seasonal cycle in the Equatorial Pacific as can be seen in Figure 5.

In the Southern Ocean and subtropical gyres, deepening nutriclines combined with the strong downwelling of the plankton to deep waters where light is limited surpresses growth in the HI-res relative to the LO-res case. This deeper mixing also provide more nutrients at the surface in the HI-res. As has been seen in all regions, the HI-res models ability to resolve vertical dynamics, which the LO-res model cannot, have a huge impact on the biogeochemical system. Thus very high concentrations of plankton in the Southern Ocean in the LO-res model which may appear to be a bias in the model may only be in fact a result of inadequate vertical dynamics. However the HI-res does not fully capture the seasonal cycle, as high chlorophyll values reappear again during the summer period, when there is a strong re-stratification, with the mixed layer depth becoming equally shallow in both the LO-res and HI-res simulations (Figure 16). In fact the high chlorophyll bias appears in many of the regions during the summer stratification. Looking at the comparison of the climatologies of the MLD in Figure 2 it is clear that both the LO-res and HI-res cases under-estimate the MLD during this period, particularly in the Southern Ocean and South Pacific. Maintaining a deeper mixed layer depth during this period may suppress the overly strong growth seen in the models during this period. This may also apply to the Equatorial region where the MLD in the model again under-estimates the observed climatology in the tropics (Figure 2(b)), though in this case throughout the entire year, which may be responsible for the higher than observed surface chlorophyll in the model.

Another factor that may be at play in determining the biases encountered within the model is the choice of biological parameters and/or functional parameterizations. While having the same values for the two cases allowed a direct intercomparison to examine the effects strictly due to the differences in resolution, it may be that some of these parameters need to be adjusted for the $1/4^\circ$ case. One example of this may be in the Southern Ocean where the HI-res has too high chlorophyll in deep waters (Figure 15). This also occurs for the subtropical gyres, where moreover there is a shift in the seasonal cycle in the HI-res relative to the observations (Figure 13). This shift is caused by an extended deep mixing period which reduces chlorophyll through light limitation, rather than nutrient availability. Thus the improved deep winter mixing alone disrupts the seasonal cycle, implying that modifications of the biological parameterizations is required in order to improve the HI-res here. In fact, more generally, parameterization of the biological model may need to be resolution dependent, so that the biogeochemical system can react appropriately to the physical system that is available to it. In the case of the LO-res this would imply having parameter values which compensate for the unresolved vertical dynamics. To achieve such a parameterization a further study of how the resolved dynamics impacts on the growth rates and community structure would need to be undertaken. While in this work the focus has been on examining the effect of resolved dynamics on nutrient supply and chlorophyll, being that these are the main currencies available for comparison with observed data, future work determining which species are particularly sensitive to these different dynamics would be crucial in any future development of model parameterizations that are resolution dependent.

As the simulation at $1/4^\circ$ resolution (HI-res) is an initialization from the LO-res biology within the HI-res physics there is an adjustment taking place. Unfortunately because of the computational cost in running the HI-res experiment a long spin up of the fully coupled model could not be performed and this is likely to affect the interpretation of the role of better resolved physics on the biogeochemistry. The LO-res experiment was originally intended to be the longer-term spin up for the HI-res, with the idea that the HI-res could provide more details on the evolution of biogeochemistry over certain target periods. However, it has become clear that the limited ability of the LO-res in the representation of vertical dynamics lead to a mean location of the nutricline that is generally much deeper than observed (see for instance Sec. 3.2.2). During the spin up and simulation years prior to 2000 of the LO-res, the nutricline is generally eroded with respect to the initial climatology from the World Ocean Atlas. This is particularly evident in the coastal upwelling regions such as the one presented in Fig. 10. The resulting state is then used by the HI-res as initial conditions, and notwithstanding the improved resolution of vertical physics, the nutricline shows a rather slow upward shift, which is in contrast with other regions such as the equatorial Pacific (and Atlantic, not shown) where the nutricline and resulting DCM are moved significantly closer to the surface and to the observations.

It is also likely that there is an ongoing slow adjustment of the nutrient surfaces. In most regions the adjustment appears to be relatively fast (< 4 months). In a sense the LO-res provides a first order approximation to the global system, but is limited by the LO-res physics which does not resolve adequately the vertical motions needed to both provide nutrients and limit light in different parts of the ocean. Using the HI-res allows an adjustment to overcome these limitations in the LO-res physics. When the adjustment timescales are relatively fast this approach may provide a cost effective means of capturing more realistic features within the biogeochemical system. However the adjustment in certain regions is still not able to overcome the initial conditions produced by the LO-res, for example in the coastal region where the under-estimated nutrient availability persists throughout the HI-res simulation.

It may thus be argued that, given the enhanced vertical physics, starting the HI-res from climatological nutrient conditions could lead to a more adequate state in a shorter period. Another issue would imply the adjustment of the remineralisation rates of the biogeochemical model in the LO-res spin up to retain nutrients closer to the surface and then verify that these new parameters are also consistent with the vertical dynamics of the HI-res. The computational limitations hamper the number of experiments that would provide answers to these questions. This simulation is certainly a preliminary step towards performing global online complex biogeochemical simulations with realistic configurations, but it is a useful step as it has the kind of resolution that will become standard in future Earth system models. In future studies, with the growing availability of more powerful computing systems, longer time integrations of the HI-res model will be performed in order to see the long term adjustment of the biogeochemical system.

Acknowledgements

This work is funded by the GreenSeas project (2010-2013) in the framework of the European Community FP7 Framework Programme. The research leading to these results has received funding from the Italian Ministry of Education, University and Research and the Italian Ministry of Environment, Land and Sea under the GEMINA project. We wish to thank Dorotea Iovino for her advice in setting up the model.

References

Arhan, M., Speich, S., Messager, C., Dencausse, G., Fine, R., Boye, M., 2011. Anticyclonic and cyclonic eddies of subtropical origin in the subantarctic zone south of Africa. *J. Geophys. Res.* *116*(C11), C11,004.

Barnier, B., Madec, G., Penduff, T., Molines, J., Treguier, A., Le Sommer, J., Beckmann, A., Biastoch, A., Boening, C., Dengg, J., Derval, C., Durand, E., Gulev, S., Remy, E., Talandier, C., Theetten, S., Maltrud, M., McClean, J., De Cuevas, B. S., Morales Maqueda, M. Á., Legat, V., Fichefet, T., 2006. Impact of partial steps and momentum advection schemes in a global ocean circulation model at eddy-permitting resolution *Ocean Dyn.* **56**, 543-567.

Blanke, B., Delecluse, P., 1993. Variability of the tropical atlantic-ocean simulated by a general-circulation model with 2 different mixed-layer physics. *J. Phys. Oceanogr.* **23**, 1363-1388.

Bouillon, S., Morales Maqueda, M. Á., Legat, V., Fichefet, T., 2009. An elastic-viscous-plastic sea ice model formulated on Arakawa B and C grids. *Ocean Modelling*, **27**, 174-184.

Conkright, M., Garcia, H., O'Brien, T., Locarnini, R., Boyer, T., Stephens, C., Antonov, J., 2002. World Ocean Atlas 2001, vol 4. *Nutrients NOAA Atlas NESDIS*, **52**, U.S. Govt. Print. Off., Washington, D.C.

Cotrim da Cunha, L., Buitenhuis, E. T., Le Quéré, C., Giraud, X., Ludwig, W., 2007. Potential impact of changes in river nutrient supply on global ocean biogeochemistry. *Global Biogeochem. Cycles*, **21**, GB4007.

Dee, D. P., Uppala, S. M., Simmons, A. J., Berrisford, P., Poli, P., Kobayashi, S., Andrae, U., Balmaseda, M. A., Balsamo, G., Bauer, P., Bechtold, P., Beljaars, A. C. M., van de Berg, L., Bidlot, J., Bormann, N., Delsol, C., Dragani, R., Fuentes, M., Geer, A. J., Haimberger, L., Healy, S. B., Hersbach, H., Hólm, E. V., Isaksen, L., Kållberg, P., Köhler, M., Matricardi, M., McNally, A. P., Monge-Sanz, B. M., Morcrette, J. J., Park, B. K., Peubey, C., de Rosnay, P., Tavolato, C., Thépaut, J. N., Vitart, F., 2011. The ERA-Interim reanalysis: configuration and performance of the data assimilation system. *Quart. J. Roy. Met. Soc.* **137(656)**, 553-597.

Doney, S. C., Lima, I., Moore, J. K., Lindsay, K., Behrenfeld, M. J., Westberry, T. K., Mahowald, N., Glover, D. M., Takahashi, T., 2009. Skill metrics for confronting global upper ocean ecosystem-biogeochemistry models against field and remote sensing data. *J. Mar. Sys.* *76*(1-2), 95–112, doi:10.1016/j.jmarsys.2008.05.015.

Ekman, V. W., 1905. On the influence of the Earth's rotation on ocean currents. *Archives of Mathematics, Astronomy and Physics*, **2(11)**, 1-53.

Fichefet, T., Morales Maqueda, M. A., 1997. Sensitivity of a global sea ice model to the treatment of ice thermodynamics and dynamics. *Geophys. Res.* **102**, 12609-12646.

Friedrichs, M. A. M., Carr, M.-E., Barber, R. T., Scardi, M., Antoine, D., Armstrong, R. A., Asanuma, I., Behrenfeld, M. J., Buitenhuis, E. T., Chai, F., Christian, J. R., Ciotti, A. M., Doney, S. C., Dowell, M., Dunne, J., Gentili, B., Gregg, W., Hoepffner, N., Ishizaka, J., Kameda, T., Lima, I., Marra, J., Melin, F., Moore, J. K., Morel, A., O'Malley, R. T., O'Reilly, J., Saba, V. S., Schmeltz, M., Smyth, T. J., Tjiputra, J., Waters, K., Westberry, T. K., Winguth, A., 2009. Assessing the uncertainties of model estimates of primary productivity in the tropical pacific ocean. *J. Mar. Sys.* *76*(1-2), 113–133, doi10.1016/j.jmarsys.2008.05.010.

Garcia, H. E., Locarnini, R. A., Boyer, T. P., Antonov, J. I., Zweng, M. M., Baranova, O. K., Johnson, D. R., 2010. World Ocean Atlas 2009, Volume 4: Nutrients (phosphate, nitrate, silicate). S. Levitus, Ed. *NOAA Atlas NESDIS 71, U.S. Government Printing Office*, Washington, D.C., 398 pp.

Gent, P. R., McWilliams, J. C., 1990. Isopycnal mixing in ocean circulation models. *J. Phys. Oceanogr.* **20**, 150-155.

Gist, N., Serret, P., Woodward, E.M.S., Chamberlain, K., Robinson, C., 2009. Seasonal and spatial variability in plankton production and respiration in the Subtropical Gyres of the Atlantic Ocean. *Deep-Sea Res. II*, **56**, 931-940.

Gregg, W. W., Conkright, M. E., Ginoux, P., O'Reilly, J. E., Casey, N. W., 2003. Ocean primary production and climate: Global decadal changes. *Geophys. Res. Lett.* **30(15)**, 1809.

Griffies, S. M., Gnanadesikan, A., Dixon, K. W., Dunne, J. P., Gerdes, R., Harrison, M. J., Rosati, A., Russell, J. L., Samuels, B. L., Spelman, M. J., Winton, M., Zhang, R., 2005. Formulation of an ocean model for global climate simulations. *Ocean Sci.* **1**, 45-79.

Gruber, N., Lechkar, Z., Frenzel, H., Marchesiello, P., Münnich, M., McWilliams, J. C., Negai, T., Plattner, G., 2011. Eddy-induced reduction of biological production eastern boundary upwelling systems. *Nature Geoscience*, **4**, 787-792.

Hosoda, S., Ohira, T., Sato, K., Suga, T., 2010. Improved description of global mixed-layer depth using Argo profiling floats. *J. Oceanogr.* **66**, 773-787.

Kang, J-H., Kim, W-S., Chang, K-L., Noh, J-H., 2004. Distribution of plankton related to the mesoscale physical structure within the surface mixed layer in the southwestern East Sea, Korea. *J. Plankton Res.* **26**, 1515-1528.

Karleskind, P., Lévy, M., Memery, L., 2011. Modifications of mode water properties by sub-mesoscales in a bio-physical model of the Northeast Atlantic. *Ocean Modelling*, **39**, 47-60.

Lathuilière, C., Echevin, V., Lévy, M., Madec, G., 2010. On the role of mesoscale circulation on an idealized coastal upwelling ecosystem. *J. Geophys. Res.*, **115**, C09018, doi:10.1029/2009JC005827.

Lathuilière, C., Lévy, M, Echevin, V., 2011. Impact of eddy-driven vertical fluxes on phytoplankton abundance in the euphotic layer. *J. Plankton Res.*, **33(5)**, 827-831, doi:10.1093/plankt/fbq131.

Le Moigne, F. A. C., Boye, M., Masson, A., Corvaisier, R., Grossteffan, E., Guéneugues, A., Pondaven, P., 2013. Description of the biogeochemical features of the subtropical southeastern atlantic and the southern ocean south of south africa during the austral summer of the international polar year. *Biogeosciences*, *10*(1), 281–295.

Levitus, S., 1982. Climatological Atlas of the global ocean *NOAA Professional Paper*, **13**, 191.

Lévy, M., 2008. The modulation of biological production by oceanic mesoscale turbulence. *Lect. Notes Phys.* **744**, 219-261.

Lévy, M., Iovino, D., Resplandy, L., Klein, P., Madec, G., Tréguier, A. -M., Masson, S., Takahashi, K., 2012. Large-scale impacts of submesososcale dynamics on phytoplankton: Local and remote effects. *Ocean Modelling*, **43-44**, 77-93.

Lévy, M., Resplandy, L., Klein, P., Capet, X., Iovino, D., Ethé, C., 2012. Grid degradation of submesoscale resolving ocean models: Benefits for offline passive tracer transport. *Ocean Modelling*, **48**, 1-9.

Lévy, M., Martin, A. P., 2013. The influence of mesoscale and submesoscale heterogeneity on ocean biogeochemical reactions. *Global Biogeochem. Cycles*, **27(4)**, 1139-1150.

Madec, G., Imbard, M., 1996. A global ocean mesh to overcome the North Pole singularity. *Clim. Dyn.* **12(6)**, 381-388.

Madec, G. Delecluse, P., Imbard, M., Levy, C., 1999. OPA8.1 ocean general circulation model reference manual. IPSL, France.

Mahadevan, A., Tandon, A., 2006. An analysis of mechanisms for submesoscale vertical motion at ocean fronts. *Ocean Modelling*, **14**, 241-256.

Mahadevan, A., Tandon, A., Ferrari, R., 2010. Rapid changes in mixed layer stratification driven by submesoscale instabilities and winds. *J. Geophy. Res.*, **115**, CO3017, doi:10.1029/2008JC005203.

Mahadevan, A., D'Asaro, E., Lee, C., Perry, M. J., 2012. Eddy-driven stratification initiates North Atlantic spring phytoplankton blooms. *Science*, **337**, 54-55.

McClain, C. R., Cleave, M. L., Feldman, G. C., Gregg, W. W., Hooker, S. B., Kuring, N., 1998. Science quality SeaWiFS data for global biosphere research. *Sea Technol.* **39**, 1016.

McClain, C. R., 2009. A decade of satellite ocean color observations. *Ann. Rev. Mar. Sci.* **1**, 1942.

McGillicuddy, D., Anderson, L., Doney, S., Maltrud, M., 2003. Eddy-driven sources and sinks of nutrients in the upper ocean: Results from a 0.1° resolution model of the north atlantic. *Global Biogeochem. Cycles*, **17(2)**, 1035.

Moore, J. K., Doney, S. C., Kleypas, J. A., Glover, D. M., Fung, I. Y., 2002. An intermediate complexity marine ecosystem model for the global domain. *Deep-Sea Res. II*, **49**, 403-462.

Nash, J., Sutcliffe, J., 1970. River flow forecasting through conceptual models, part 1 - a discussion of principles. *J. Rev. Hydrol.* **10**, 282-290.

Oke, P. R., Griffin, D. A., Schiller, A., Matear, R. J., Fiedler, R., Mansbridge, J., Lenton, A., Cahill, M., Chamberlain, M. A., 2013. Evaluation of a near-global eddy-resolving ocean model. *Geosci. Model Dev.* **6**, 591-615.

Orsi, A. H., Whitworth III, T., Worth, D. N. Jr., 1995. On the meridional extent and fronts of the Antarctic Circumpolar Current. *Deep-Sea Res. I*, **42**, 641-673.

Oschlies, A., 2002. Can eddies make ocean deserts bloom. *Global Biogeochem. Cycles*, *16*, 1106.

Palter, J. B., Lozier, M. S., 2008. On the source of Gulf Stream nutrients. *J. Geophy. Res.* **113**, C06018, doi:10.1029/2007JC004611.

Pastor, M. V., Palter, J. B., Pelegrí, J. L., Dunne, J. P., 2013. Physical drivers of interannual chlorophyll variability in the eastern subtropical North Atlantic. *J. Geophy. Res.* **118**, 3871-3886.

Pelegrí, J. L., Csanady, G. T., 1991. Nutrient transport and mixing in the Gulf Stream *J. Geophys. Res.* **96(C2)**, 2577-2583, doi:10.1029/90JC02535.

Pelegrí, J. L., Arístegui, J., Cana, L., González-Dávila, M., Hernández-Guerra, A., Hernández-León, S., Marrero-Díaz, A., Montero, M. F., Sangrà, P., Santana-Casiano, M., 2005. Coupling between the open ocean and the coastal upwelling region off northwest Africa: water recirculation and offshore pumping of organic matter. *J. Mar. Syst.* **54**, 3-37.

Pelegrí, J. L., Marrero-Díaz, A., Ratsimandresey, A., 2006. Nutrient irrigation of the North Atlantic. *Progr. Oceanogr.* **70**, 366-406.

Pennington, J., Mahoney, K., Kuwahara, V., Kolber, D., Calienes, R., Chavez, F., 2006. Primary production in the eastern tropical pacific: a review, *Prog. Oceanogr. 69*, 285–317.

Saba, V. S., Friedrichs, M. A. M., Carr, M.-E., Antoine, D., Armstrong, R. A., Asanuma, I., Aumont, O., Bates, N. R., Behrenfeld, M. J., Bennington, V., Bopp, L., Bruggeman, J., Buitenhuis, E. T., Church, M. J., Ciotti, A. M., Doney, S. C., Dowell, M., Dunne, J., Dutkiewicz, S.,

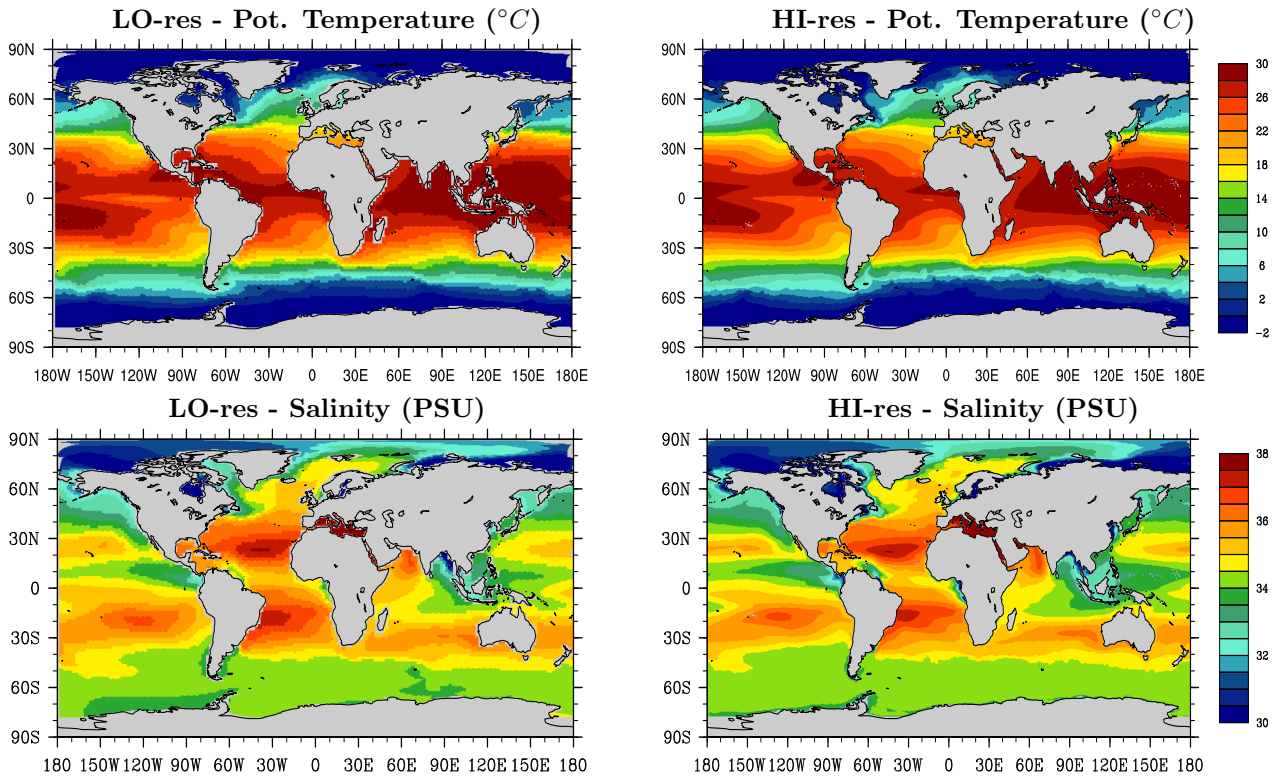

Figure 1: Colourmaps of the mean sea surface temperature (top row) and salinity (bottom row) for the LO-res (left) and HI-res (right) simulations.

Gregg, W., Hoepffner, N., Hyde, K. J. W., Ishizaka, J., Kameda, T., Karl, D. M., Lima, I., Lomas, M. W., Marra, J., McKinley, G. A., MÈlin, F., Moore, J. K., Morel, A., O'Reilly, J., Salihoglu, B., Scardi, M., Smyth, T. J., Tang, S., Tjiputra, J., Uitz, J., Vichi, M., Waters, K., Westberry, T. K., Yool, A., 2010. Challenges of modeling depth-integrated marine primary productivity over multiple decades: A case study at bats and hot. *Global Biogeochem. Cycles*, *24*(3), doi:10.1029/2009GB003655.

Schlitzer, R., 2013. Ocean Data View, http://odv.awi.de.

Srokosz, M. A., 1997. Plankton Patchiness Studies by Ship and Satellite (P^2S^3), RRS Discovery Cruise 227, SOC Cruise Report, No.12, 76 pp, 1997. *SOC Cruise Report*, **12**, 76.

Swart, S., Thomalla, S., Monteiro, P., Ansorge, I., 2012. Mesoscale features and phytoplankton biomass at the GoodHope line in the Southern Ocean during austral summer. *African J. of Mar. Sci.* **34**(4), 511–524, doi:10.2989/1814232X.2012.749811.

Troupin, C., Barth, A., Sirjacobs, D., Ouberdous, M., Brankart, J. M., Brasseur, P., Rixen, M., Alvera-Azcárate, A., Belounis, M., Capet, A., Lenartz, F., Toussaint, M. E., Beckers, J. M., 2012. Generation of analysis and consistent error fields using the Data Interpolating Variational Analysis (DIVA), *Ocean Modelling*, *52–53*(0), 90–101, 10.1016/j.ocemod.2012.05.002.

Vichi, M., Pinardi, N., Masina, S., 2007. A generalized model of pelagic biogeochemistry for the global ocean ecosystem. Part I: Theory. *J. Mar. Syst.* **64(1-4)**, 89-109.

Vichi, M., Masina, S., Navarra, A., 2007. A generalized model of pelagic biogeochemistry for the global ocean ecosystem. Part II: Numerical simulations. *J. Mar. Syst.* **64(1-4)**, 110-134.

Vichi, M., Masina, S., 2009. Skill assessment of the PELAGOS global ocean biogeochemistry model over the period 1980-2000. *Biogeosciences*, **6**, 2333-2353.

Vichi, M., Allen, J. I., Masina, S., Hardman-Mountford, N. J., 2011. The emergence of ocean biogeochemical provinces: A quantitative assessment and a diagnostic for model evaluation. *Biogeosciences*, **25**, GB2005.

Vichi, M., Gutierrez-Mlot, E., Lazzari, P., Lovato, T., Mattia, G., McKiver, W., Masina, S., Pinardi, N., Solidoro, C., Zavatarelli, M., 2014. The Biogeochemical Flux Model (BFM): Equation Description and User Manual. BFM version 5.1 (BFM-V5). Release 1.1. *BFM Report Series 1*, Bologna, Italy, http://bfm-community.eu.

Vogt, M., Vallina, S. M., Buitenhuis, E. T., Bopp, L., Le Quéré, C., 2010. Simulating dimethylsulphide seasonality with the Dynamic Green Ocean Model PlankTOM5. *J Geophys. Res.* **115**, CO6021.

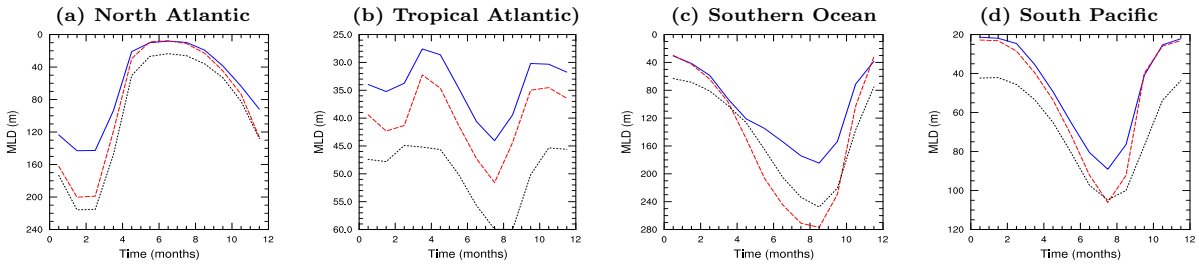

Figure 2: Climatologies of the average MLD in the (a) North Atlantic (from latitude 25N to 70N and longitude 80W to 10E), (b) Tropical Atlantic (latitude -25S to 25N, longitude 70W to 20E), (c) Southern Ocean (south of 45S) and (d) the South Pacific (from latitude -45S to 0, longitude 180W to 70W) for the LO-res (blue) and HI-res (red dashed line) simulations, plus the observed climatologies from Argo data (*Hosoda et al*. [2010], black dotted line).

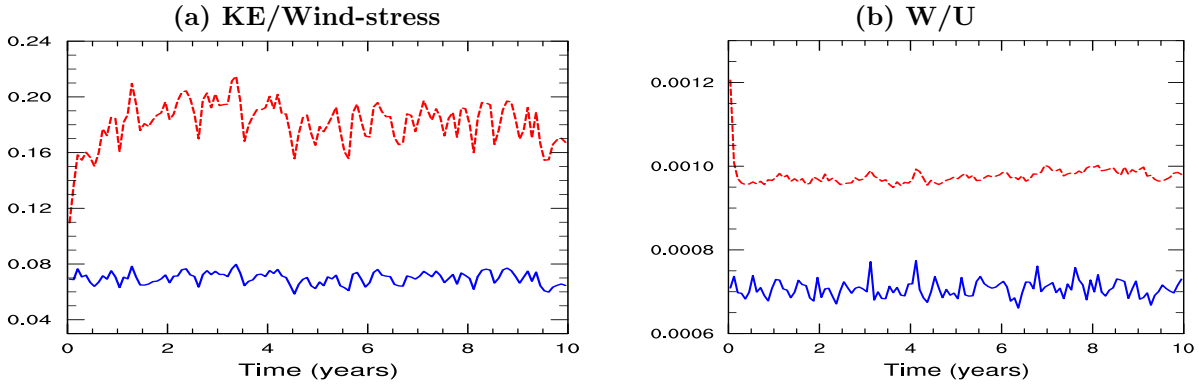

Figure 3: Timeseries of the globally averaged (a) ratio of the kinetic energy and the wind stress and (b) the ratio of the magnitude of the vertical velocity to the horizontal velocity for the spinup of the LO-res (blue) and HI-res (red) simulations.

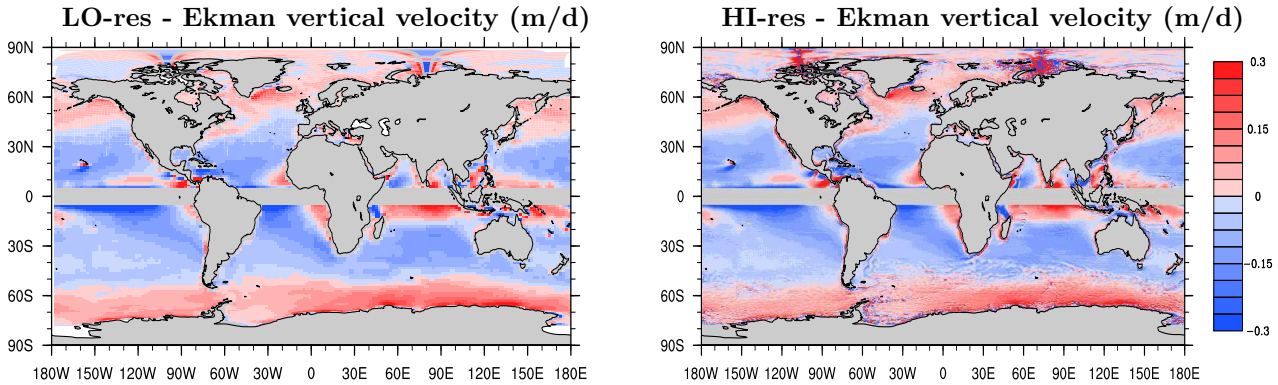

Figure 4: Colourmaps of the mean Ekman induced vertical velocity for the LO-res (left) and HI-res (right) simulations. Red indicates Ekman suction (upwelling) whereas blue indicates Ekman pumping (downwelling).

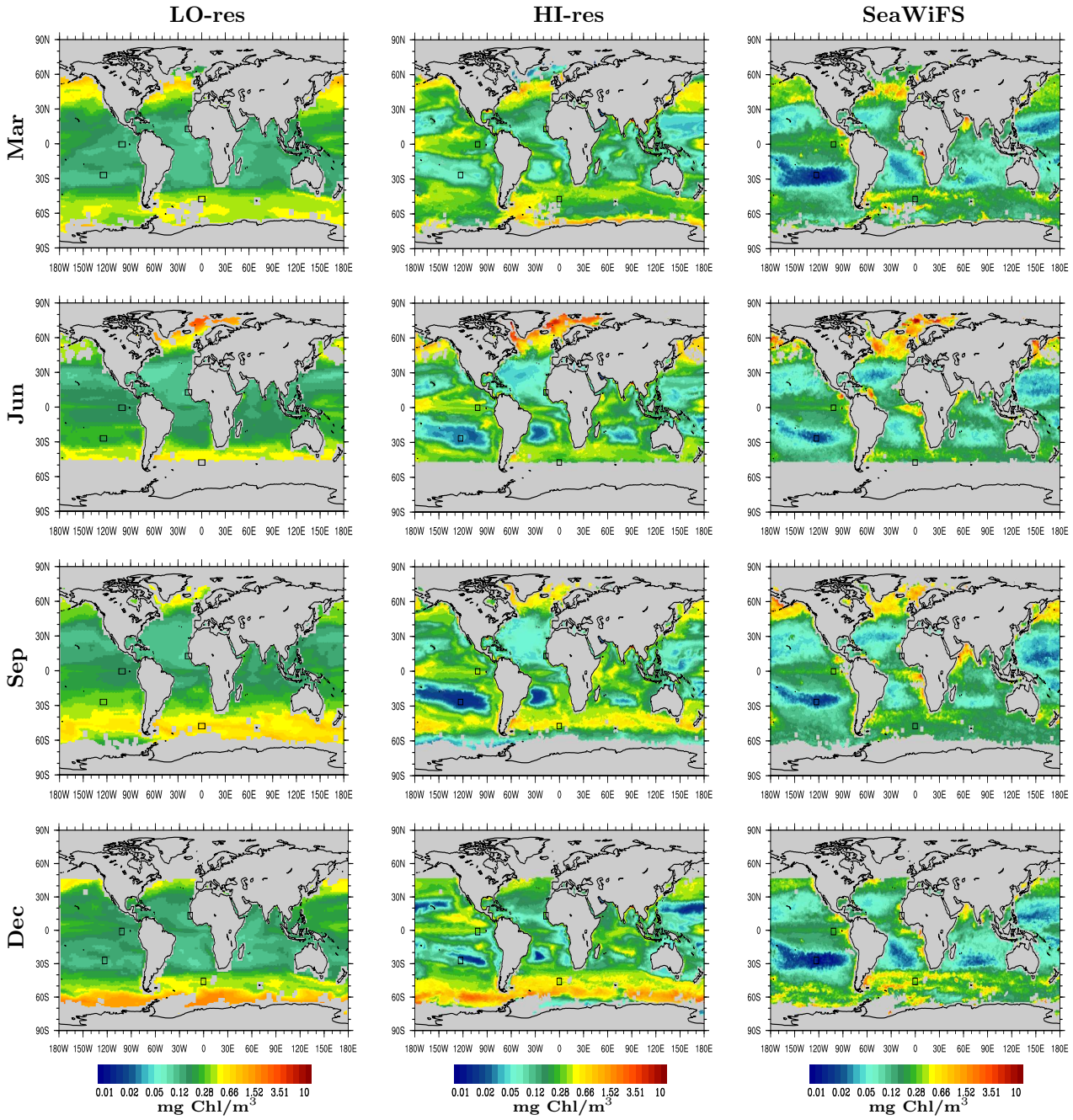

Figure 5: Colourmaps of the monthly mean surface chlorophyll in the LO-res (left column) and HI-res (middle column) simulations as well as SeaWiFS observations (right colum) for March (top), June (2nd row), September (3rd row) and December (4th row) 2000, with the equivalent SeaWiFS maps (right). Note that grey indicates not only land points but also missing values in the SeaWiFS colourmaps. The boxes indicated show the 4 regions where timeseries are extracted.

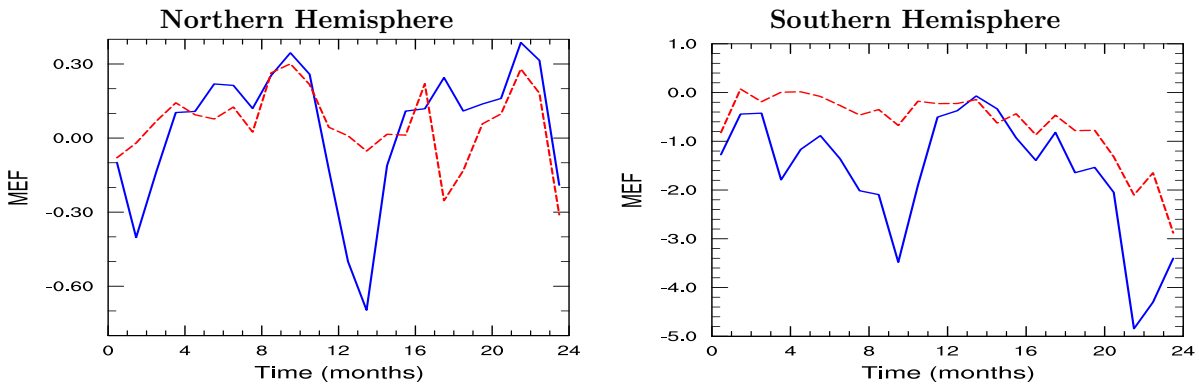

Figure 6: Timeseries (from January 1999) of the Model Efficiency (MEF) index computed in the Northern (left) and Southern (right) Hemisphere for the LO-res (blue) and HI-res (red) monthly mean surface chlorophyll compared with the SeaWiFS satellite observations.

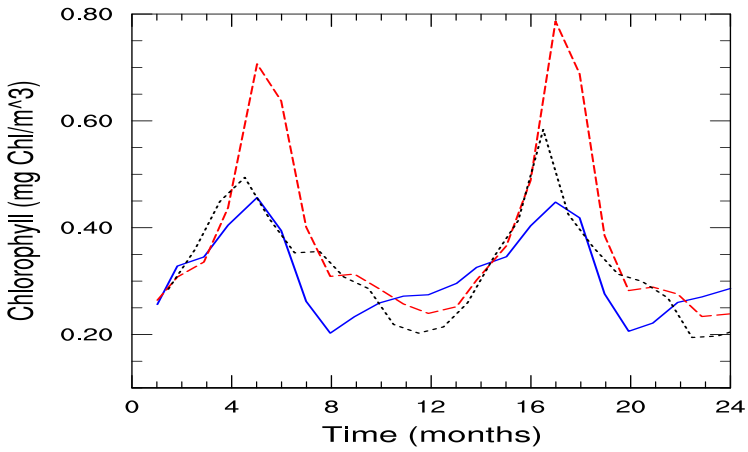

Figure 7: Timeseries (from January 1999) of surface chlorophyll averaged in the North Atlantic (from latitude 25°N to 70°N and longitude 80°W to 10°E) for the LO-res (blue) and HI-res (red) simulations, and for SeaWiFS data (black).

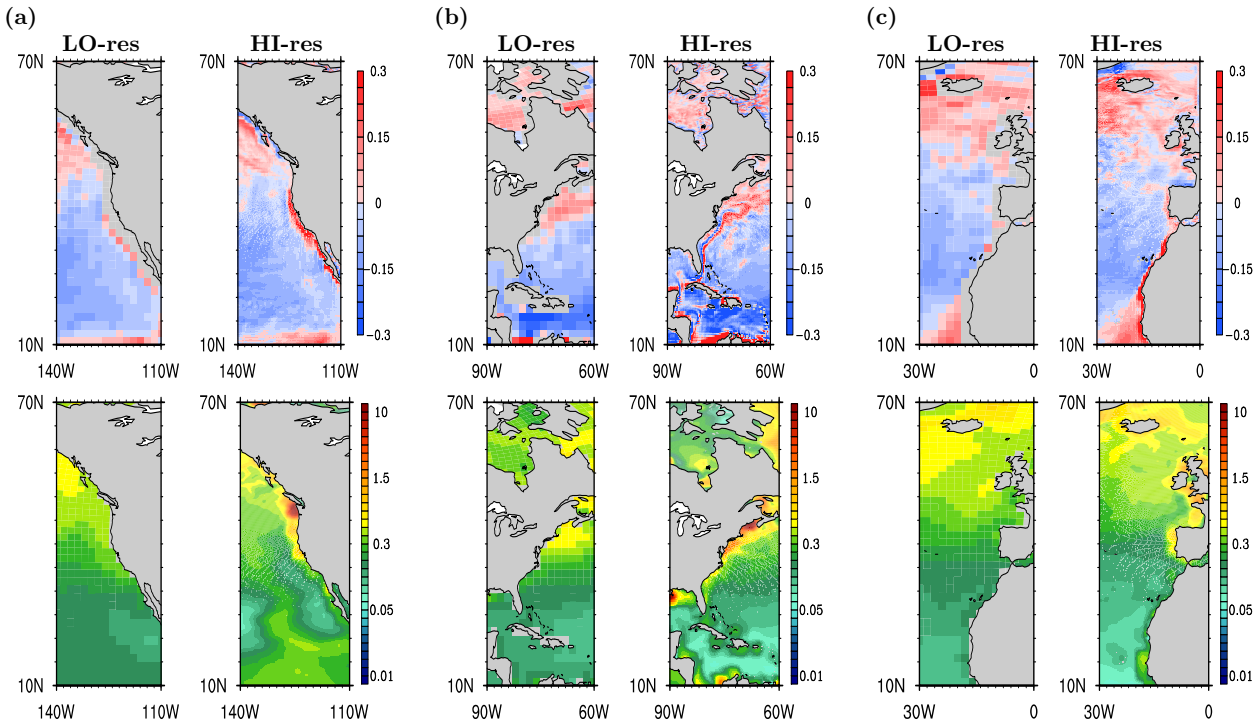

Figure 8: Colourmaps of the annual mean value of the Ekman vertical velocity (top) and chlorophyll (bottom) in three coastal regions (a) Eastern North Pacific, (b) Western North Atlantic and (c) Eastern North Atlantic. Note that the land-sea mask is different for the Ekman and chlorophyll cases.

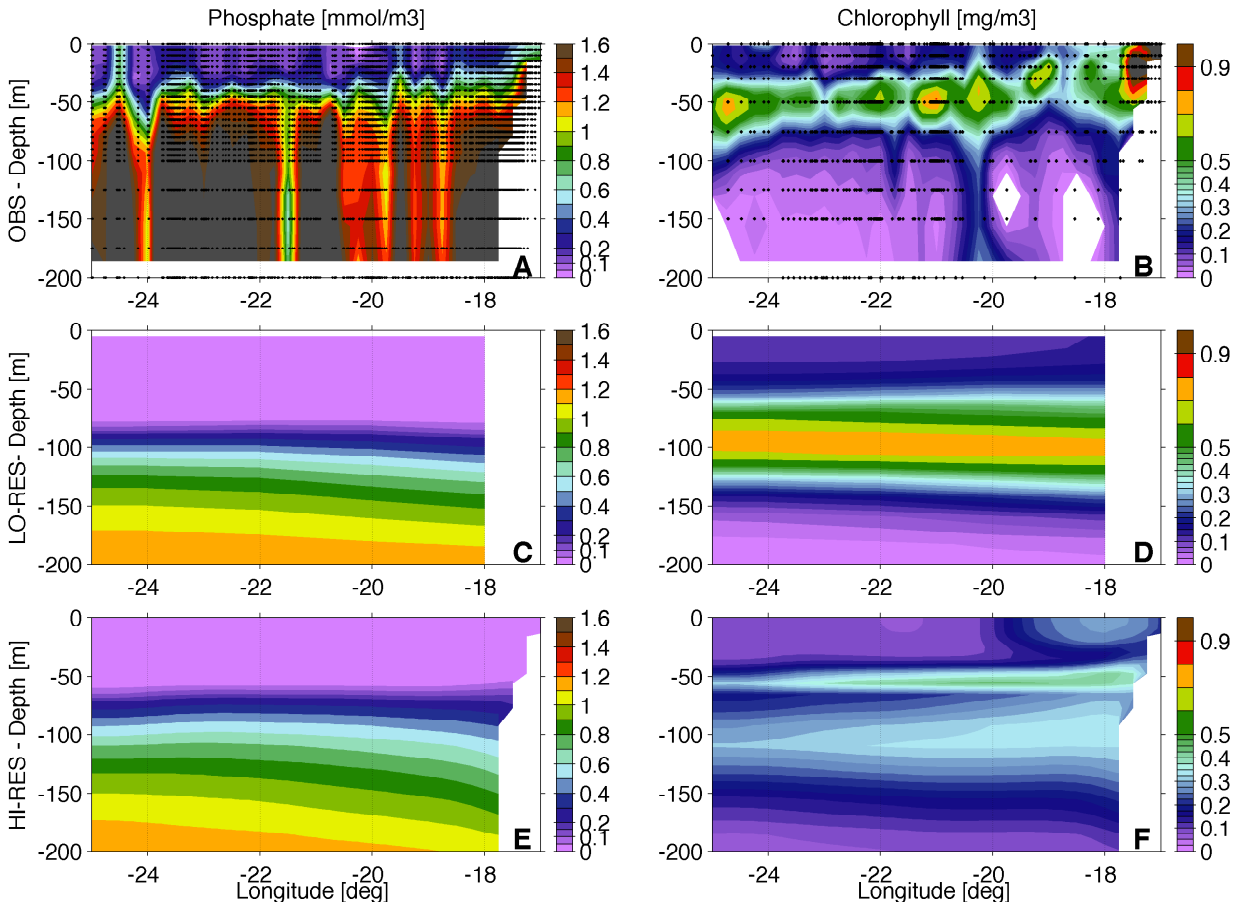

Figure 9: Coastal Atlantic cross sections taken at 13°N of the annual mean values of phosphate (left column) and chlorophyll (right column) from observations (top row), as well as the LO-res (2nd row) and HI-res (bottom row) simulations. Data have been obtained from the World Ocean Database 2013 with an interval of 1° around the section and objectively analyzed on the HI-res model grid using Ocean Data View *Schlitzer* [2013] and the DIVA gridding tool (*Troupin et al*. [2012]).

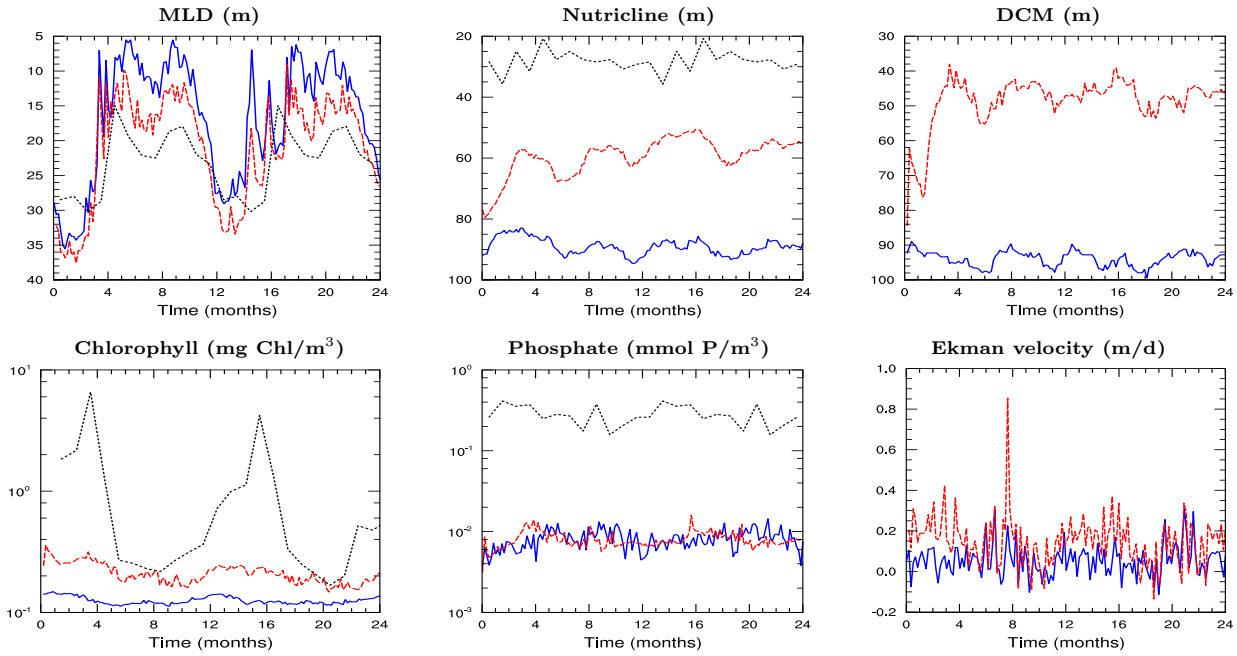

Figure 10: Coastal Atlantic timeseries (from January 1999) of quantities averaged in a $6^\circ \times 6^\circ$ box centered at (18°W, 13°N). The blue and red lines indicate LO-res and HI-res cases respectively. The bottom row are concentrations at the surface, and the Ekman velocity is the wind induced vertical velocity computed from the curl of the wind stress. In the case of the MLD, chlorophyll and phosphate we include observation data for comparison, the Argo climatology, SeaWiFS and WOA data respectively (black lines). The simulation data are 5 day snapshots while the observed chlorophyll are monthly averaged values, while the MLD and phosphate are climatologies.

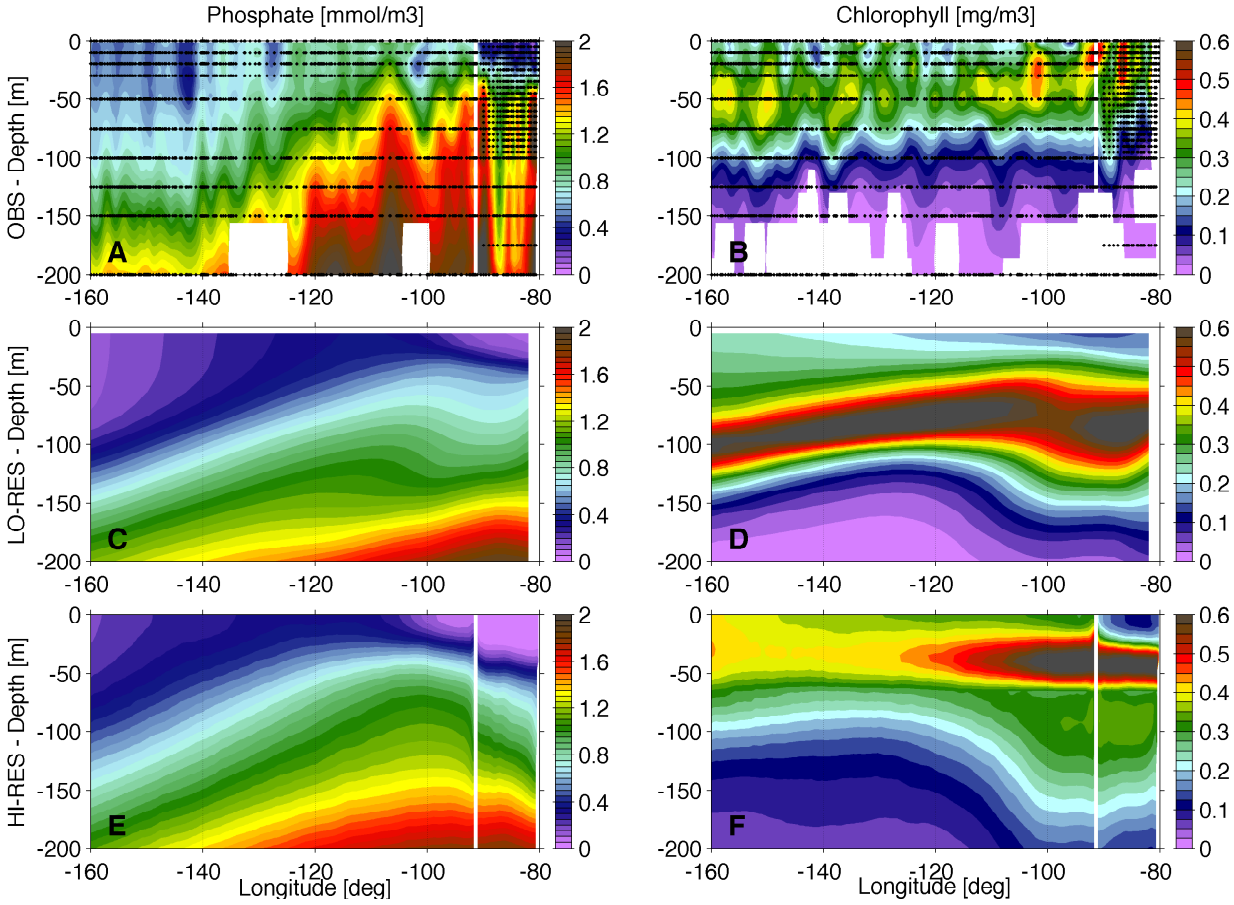

Figure 11: Equatorial cross sections in the eastern Pacific Ocean of the annual mean values of phosphate (left column) and chlorophyll (right column) from observations (top row), as well as the LO-res (2nd row) and HI-res (bottom row) simulations. Data have been obtained from the World Ocean Database 2013 with an interval of 1° around the equator and objectively analyzed on the HI-res model grid using Ocean Data View *Schlitzer* [2013] and the DIVA gridding tool (*Troupin et al*. [2012]).

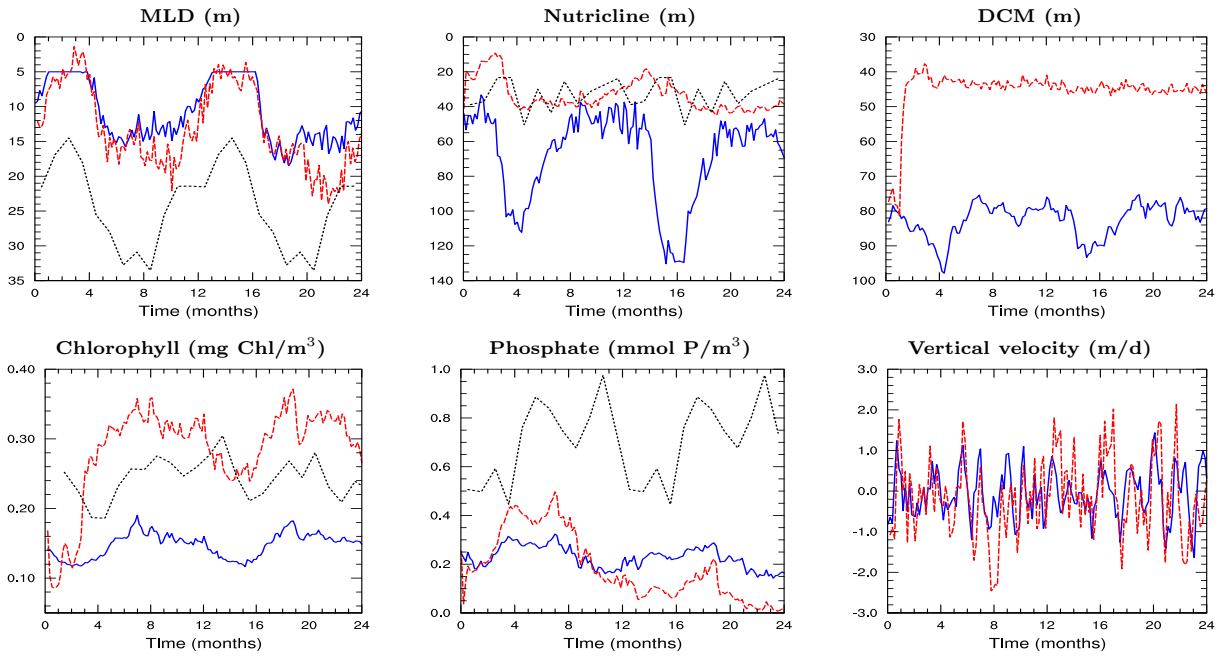

Figure 12: As in Fig. 10 but now for a box centered at 100°W, 0N in the equatorial Pacific. The chlorophyll and phosphare are concentrations at the surface, whereas the vertical velocity is averaged over depth of the water column.

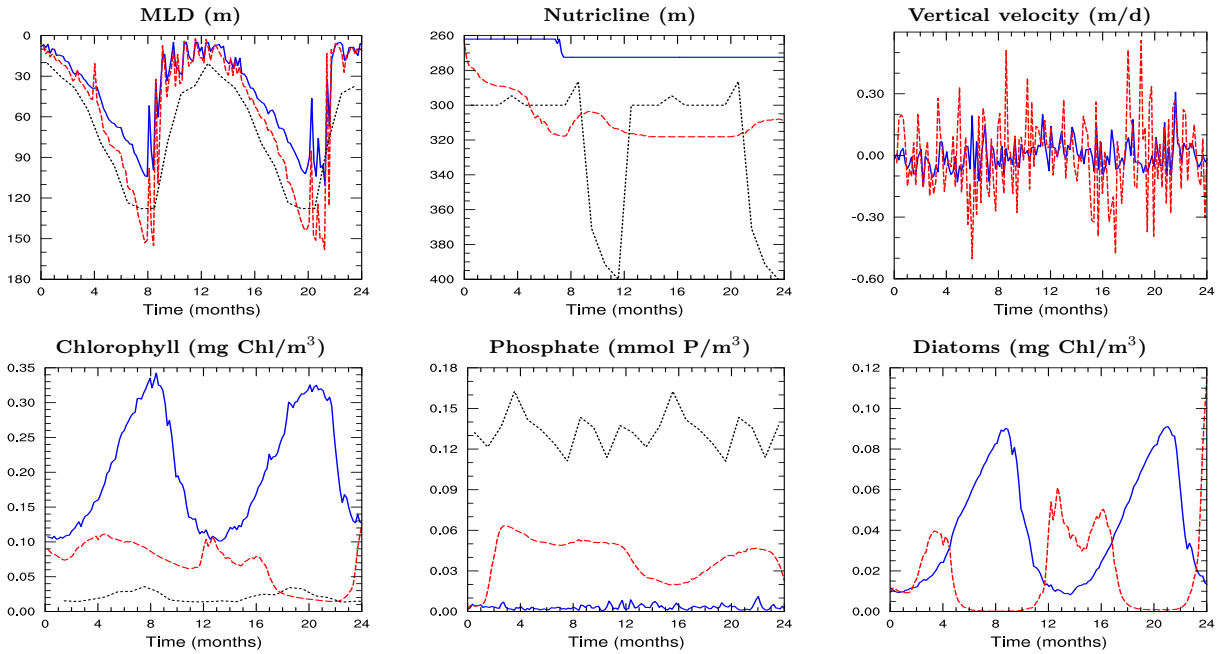

Figure 13: As in Figure 12 but now for a box centered at 123°W, 27S in the Southern Pacific subtropical gyre.

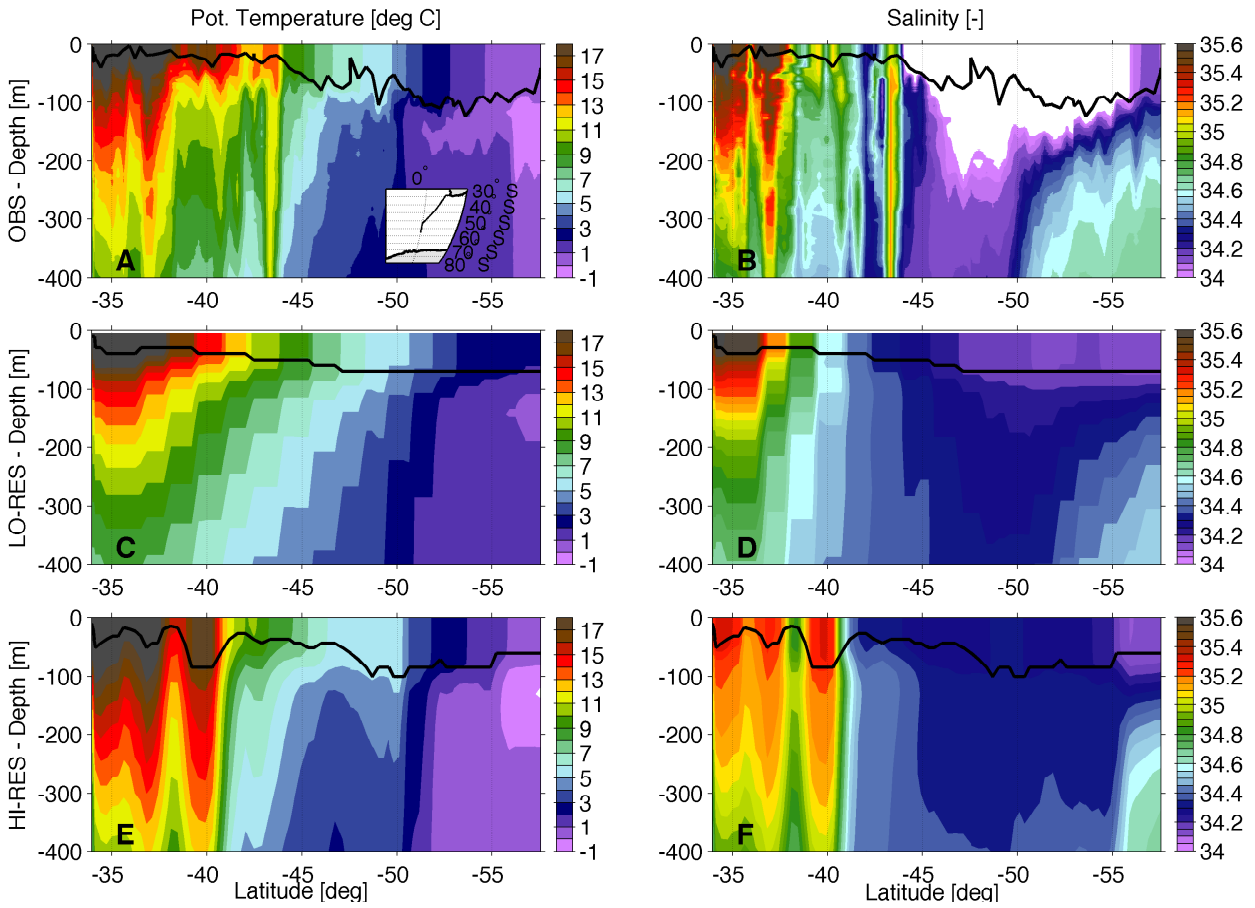

Figure 14: Depth profiles of temperature and salinity along transect crossing the Southern Ocean front of the LO-res (2nd row), HI-res (bottom row) and measured in-situ data (top row). The mixed layer depth (continuous black line) was computed with a 0.01 σ_t density criterium both for the data and models. Data have been objectively analyzed on the HI-res model grid using Ocean Data View (*Schlitzer* [2013]) and the DIVA gridding tool (*Troupin et al*. [2012]). Blank values have been masked because found below the quality limit for the objective analysis.

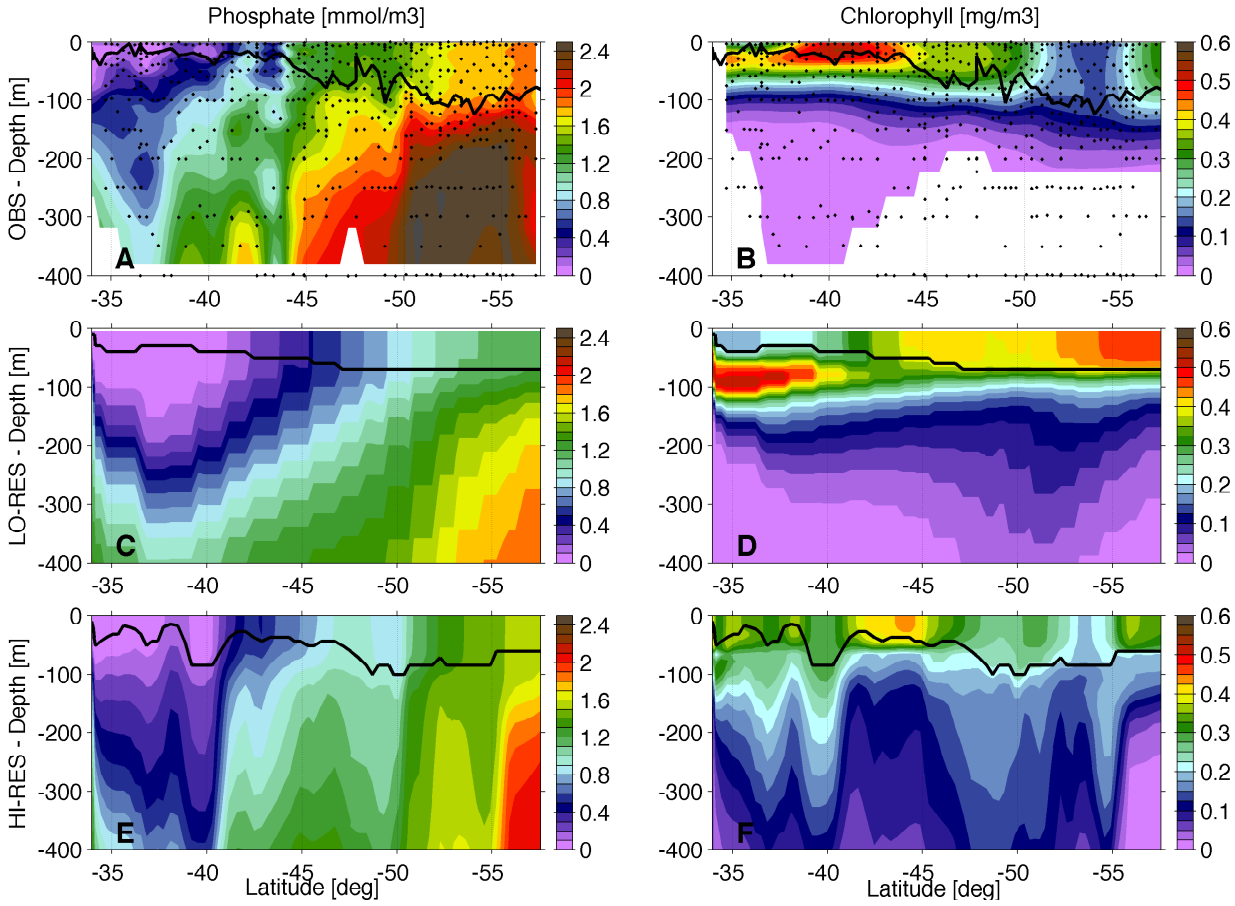

Figure 15: As in Figure 14 but now for phosphate and chlorophyll. Data have been objectively analyzed on the HI-res model grid using Ocean Data View (*Schlitzer* [2013]) and the DIVA gridding tool (*Troupin et al*. [2012]) .

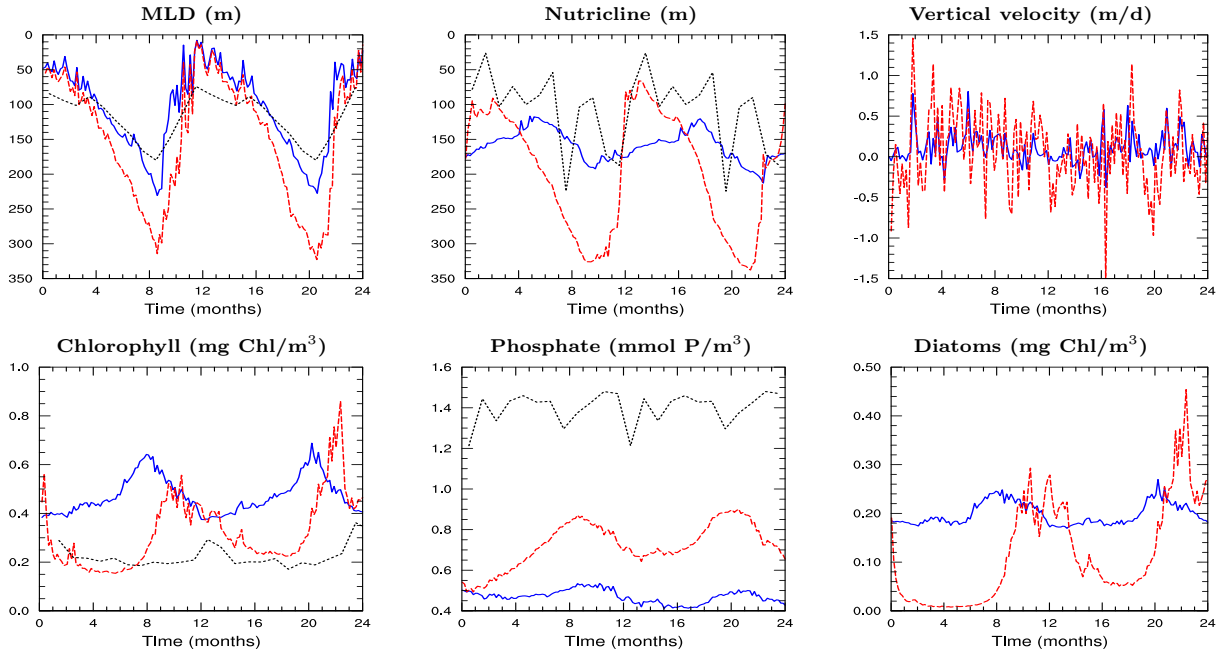

Figure 16: As in Figure 13 but now for a box centered at 0°W, 46S at the Southern Ocean front.